

Cite this: *Energy Environ. Sci.*,  
2026, 19, 264

## Decarbonizing potential of global container shipping with hydrogen-based fuels

Shijie Wei, \*<sup>a</sup> Arnold Tukker<sup>ab</sup> and Bernhard Steubing <sup>a</sup>

Hydrogen-based fuels are expected to support maritime shipping in reaching net-zero climate targets. However, the complexity of hydrogen-based fuel supply, propulsion system deployment, and fleet composition make their full life cycle decarbonization potential unclear. A comprehensive fleet-level assessment of their decarbonization potential is thus essential. Here, we evaluate the life cycle climate change impact of global container shipping using hydrogen-based fuels from 2020 to 2050, considering fuel mix, propulsion system, ship size and transport demand. By integrating energy scenarios from the International Energy Agency with socio-economic scenarios from the Shared Socioeconomic Pathways and the Organization for Economic Co-operation and Development, we explore three scenarios that represent different levels of ambition for the future hydrogen production transition, hydrogen-based fuel use, and corresponding transport demand: the Less Ambitious, Ambitious and Very Ambitious scenarios. Our findings indicate that container shipping's greenhouse gas (GHG) emissions per tonne-nautical mile could decrease from 22 g CO<sub>2</sub>-eq in 2020 to 21 g, 9 g, and 3 g CO<sub>2</sub>-eq by 2050 under the Less Ambitious, Ambitious, and Very Ambitious scenarios, respectively. Cumulative GHG emissions from global container shipping could reach 9–12 Gt, 7–10 Gt, and 4–5 Gt CO<sub>2</sub>-eq between 2020 and 2050 across these scenarios, accounting for 1–3% of the global carbon budget required to achieve the worldwide net-zero target. The substitution of heavy fuel oil with hydrogen-based fuels does not always lead to a reduction in GHG emissions: in the Less Ambitious scenario, cumulative emissions increase by 0.4–0.6 Gt CO<sub>2</sub>-eq due to the slow decarbonization in hydrogen production, whereas in the Ambitious and Very Ambitious scenarios, they decline by 1–2 Gt and 3–5 Gt CO<sub>2</sub>-eq, respectively. Deep decarbonization of maritime shipping requires overcoming key bottlenecks in renovating the fleet, scaling up ammonia production and electrolyzer capacity, and ensuring sufficient renewable electricity supply. This highlights the need for coherent policies to foster multi-sectoral coordination among maritime shipping, hydrogen-based fuel production, and power generation to maximize their decarbonizing potential.

Received 20th June 2025,  
Accepted 25th November 2025

DOI: 10.1039/d5ee03477a

rsc.li/ees

### Broader context

Hydrogen-based fuels are gaining attention as a key solution for decarbonizing the maritime shipping sector. Yet, the full life-cycle decarbonization potential of these fuels remains uncertain, primarily due to the complexity of the sector. A comprehensive assessment framework is necessary to quantify this potential. The prospective life cycle assessment that integrates technological details with broader socioeconomic developments can provide a clearer understanding of hydrogen-based fuels' role in maritime shipping. Such an approach can also help guide the International Maritime Organization and policymakers in shaping effective decarbonization roadmaps. This paper also highlights the potential challenges of relying on hydrogen-based fuels for deep decarbonization in the shipping sector.

## 1. Introduction

Maritime shipping enables more than 80% of global merchandise trade by volume and accounted for 2% of annual global

greenhouse gas (GHG) emissions, totaling 1.01 Gt carbon dioxide equivalent (CO<sub>2</sub>-eq) in 2022, primarily due to its reliance on fossil fuels such as heavy fuel oil (HFO) and marine gas oil (MGO).<sup>1,2</sup> If left unregulated, these emissions could rise to as much as 1.5 Gt CO<sub>2</sub>-eq by 2050.<sup>3</sup> The International Maritime Organization (IMO) has set a strategic and guidance-based target to achieve net-zero GHG emissions from international shipping by 2050.<sup>4</sup> The maritime shipping sector faces an urgent need for decarbonization, but the transition path is

<sup>a</sup> Institute of Environmental Sciences (CML), Leiden University, 2333 CC Leiden, The Netherlands. E-mail: s.j.wei@cml.leidenuniv.nl

<sup>b</sup> The Netherlands Organization for Applied Scientific Research TNO, The Netherlands



fraught with uncertainties.<sup>5,6</sup> Low-carbon hydrogen (H<sub>2</sub>)-based fuels, *e.g.*, H<sub>2</sub>, ammonia (NH<sub>3</sub>) and methanol (MeOH), have the potential to reduce the GHG emissions from ships featuring their high technology readiness level and feedstock availability.<sup>7–10</sup> The adoption of these alternative fuels is further encouraged by regional policies such as the FuelEU Maritime Regulation under the EU's Fit for 55 package.<sup>11</sup>

However, given the complexity in H<sub>2</sub>-based fuel supply, propulsion system deployment, and fleet composition, the life-cycle decarbonization potential of H<sub>2</sub>-based fuels in maritime shipping is not well understood. Specifically, the production of H<sub>2</sub>-based fuels is not carbon-free, and their GHG emissions vary depending on the feedstock, such as fossil fuels, biomass, and electricity.<sup>12–15</sup> Moreover, the H<sub>2</sub> production mix exhibits temporal and regional variations.<sup>12</sup> For propulsion systems, H<sub>2</sub>-based fuels can be used in internal combustion engines (ICE), which has lower costs, or in fuel cells such as proton-exchange membrane fuel cells (PEMFC) and solid oxide fuel cells (SOFC), which offer higher efficiencies (55% and 60%, respectively) and zero GHG emissions.<sup>16</sup> Other alternative propulsion systems, such as ICE fueled by liquefied natural gas (LNG), biofuels, and batteries, can also play a role alongside H<sub>2</sub>-based fuels.<sup>10,17</sup> The use of LNG, batteries, and H<sub>2</sub>-based fuels affects cargo capacity due to their lower volumetric and gravimetric energy densities (by 60–97% and 14–98%, respectively) compared to conventional fuels.<sup>7,18,19</sup> Furthermore, GHG emissions per transport work decrease as ship size increases, due to the economies of scale.<sup>3</sup> The future transport demand and the composition of ship sizes will also influence the decarbonization potential of H<sub>2</sub>-based fuels.

While previous studies have examined the life cycle GHG emissions reduction potential of H<sub>2</sub>-based fuels at the individual ship level by life cycle assessment (LCA),<sup>20–23</sup> they have primarily focused on single fuel types within a specific country or region. This hinders a comprehensive understanding of the decarbonization potential of H<sub>2</sub>-based fuels in the maritime shipping sector from a systematic and global perspective. In this study, we quantify the life cycle decarbonizing potential of hydrogen-based fuels in global container shipping at both the individual ship and fleet levels from 2020 to 2050. Our analysis accounts for fuel mixes, propulsion systems, ship sizes, and transport demand. We consider three scenarios representing different levels of ambition for hydrogen-based fuel and propulsion system adoption. This study clarifies the role of H<sub>2</sub>-based fuels in decarbonizing global container shipping and can effectively inform policymakers in shaping decarbonization roadmaps.

## 2. Methods and data

### 2.1. Goal and scope

Using attributional LCA, this paper aims to assess the climate change impact caused by key propulsion systems for global container shipping from 2020 to 2050, using both one tonne-nautical mile (t-nm) and the future global containerized

transport demand as functional unit. Adopting a cradle-to-grave scope, a first functional unit is defined as carrying one tonne of cargo over a distance of one nautical mile. We further calculate impacts for a second functional unit, defined as total global containerized transport demand, according to scenarios further elaborated below.

As shown in Fig. 1, nine propulsion systems are considered: ICE fueled by HFO, ICE fueled by LNG, ICE fueled by liquefied biomethane (bio-LNG), battery, ICE fueled by liquid H<sub>2</sub>, PEMFC fueled by liquid H<sub>2</sub>, ICE fueled by liquid NH<sub>3</sub>, SOFC fueled by liquid NH<sub>3</sub>, and ICE fueled by MeOH. Currently, HFO-ICE and LNG-ICE have been commercially deployed. Bio-LNG-ICE and MeOH-ICE are already used in shipping in small quantities (technology readiness level, TRL 9) and are expected to reach full commercialization by the late 2020s.<sup>24</sup> Battery systems are also at TRL 9, but their large-scale application in international shipping remains limited.<sup>24</sup> Liquid H<sub>2</sub>-ICE and liquid NH<sub>3</sub>-ICE are still at the demonstration stage (TRL 7–8) and are expected to be fully commercialized in the mid-2030s.<sup>24</sup> Liquid H<sub>2</sub>-PEMFC is at TRL 8, while liquid NH<sub>3</sub>-SOFC is at TRL 6–7.<sup>24,25</sup> Fuel cell propulsion systems are projected to achieve full commercialization around 2040.<sup>24</sup> The foreground life cycle inventory (LCI) data for these systems are based on ship designs and operational conditions across nine ship sizes (see Sections 2.2.1 and 2.2.3). For H<sub>2</sub> production, nine technological pathways are evaluated (see Section 2.2.2). Future transport demand for global container shipping through 2050, along with the distribution of ship sizes and propulsion system shares, is informed by three scenarios: the Less Ambitious, Ambitious, and Very Ambitious Scenarios (see Section 2.2.4). The detailed LCA methodology is described in the following sections.

### 2.2. Life cycle inventories analysis

In this study, nine size categories of container ships, ranging from 0–999 TEU to 20 000+ TEU, as classified in the IMO's Fourth Greenhouse Gas Report,<sup>3</sup> are considered. The contribution of different ship sizes to global containerized transport demand over time is shown in Fig. S2 in the SI. For each ship size, based on the average deadweight tonnage and installed main engine power summarized in the IMO's report, a representative ship is chosen as the prototype to design the ship propulsion systems and assess GHG emissions from ship operation using different alternative fuels. Specific ship information (*i.e.*, deadweight tonnage, main engine power, auxiliary engine power, and fuel tank size) and operation parameters (*i.e.*, range, draught and speed), are collected from the open-source ship database *Scheepvaartwest*<sup>26</sup> and from Automatic Identification System (AIS) data *via myShipTracking*,<sup>27</sup> respectively. For each representative ship, the operation data from multiple ships of the same type is cross-checked to ensure its rationality. The full set of parameters for the nine ships can be found in Table S1 of the SI.

Here, we will discuss the unit process data for ship production, fuel supply, ship operation and future transport demand. All unit process data can be found in Section 1 of the SI.



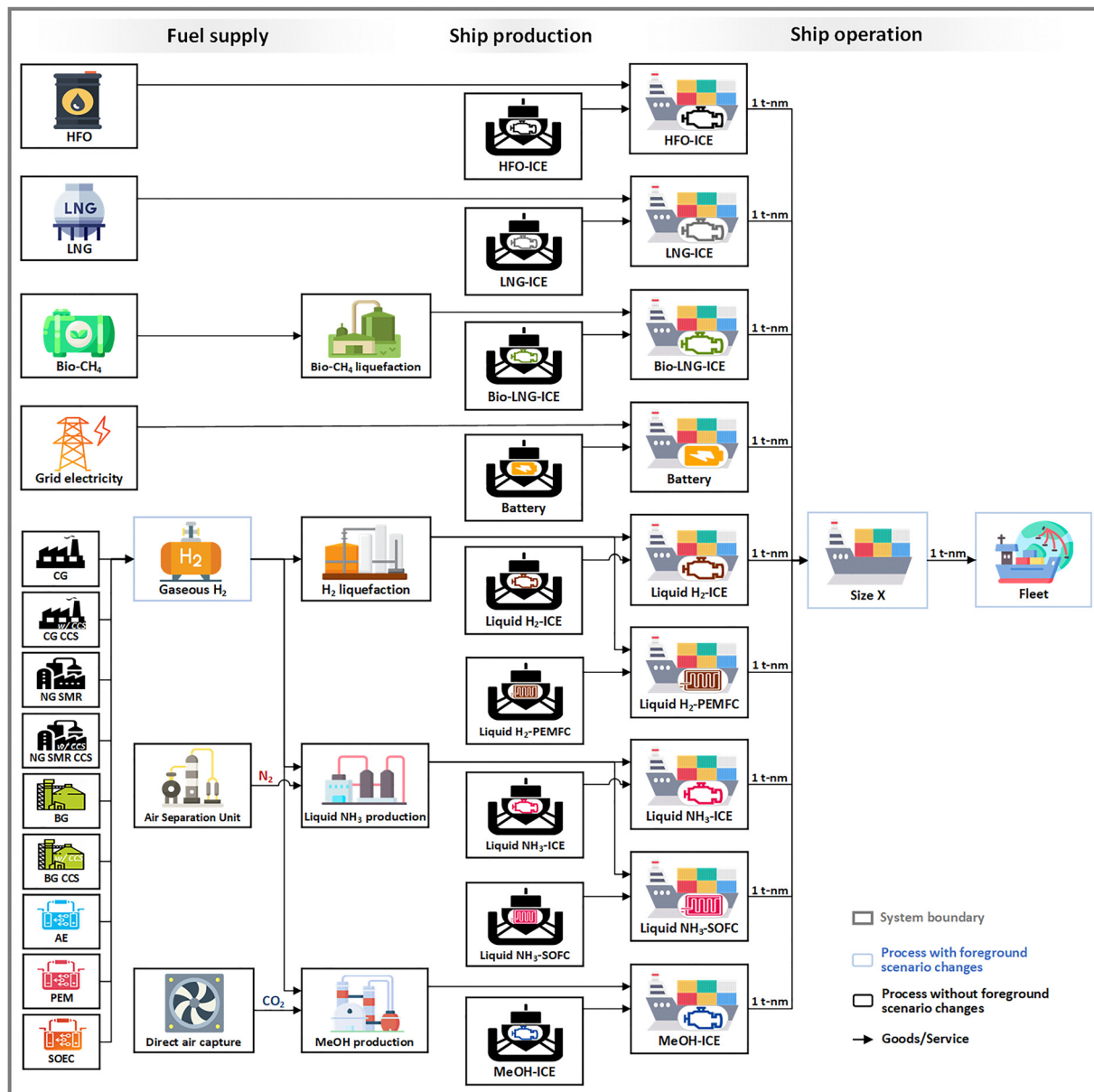


Fig. 1 The LCA model of container shipping.<sup>†</sup> In this figure, CG = coal gasification, NG SMR = steam methane reforming of natural gas, BG = biomass gasification, CCS = carbon capture and storage, AE = alkaline electrolyzers, PEM = proton exchange membrane electrolyzers, SOEC = solid oxide electrolysis cells, ICE = internal combustion engines, PEMFC = proton-exchange membrane fuel cells, SOFC = solid oxide fuel cells, HFO = heavy fuel oil, LNG = liquefied natural gas, and Bio-LNG = liquefied biomethane. Nine ship size categories are considered. For LNG-ICE, Bio-LNG-ICE, liquid H<sub>2</sub>-ICE, liquid NH<sub>3</sub>-ICE, and MeOH-ICE, a small amount of marine gas oil is required as pilot fuel. Size X represents nine container ship categories with capacities ranging from 0–999 TEU, 1000–1999 TEU, 2000–2999 TEU, 3000–4999 TEU, 5000–7999 TEU, 8000–11 999 TEU, 12 000–14 499 TEU, 14 500–19 999 TEU, and 20 000+ TEU. TEU (twenty-foot equivalent unit) refers to a standard 20-foot-long shipping container. Battery-powered ships are only applicable to the 0–999 TEU category.

### 2.2.1. Ship production

**Hull production.** For different sizes of container ships, the material requirements for hull production are determined by the lightweight mass, as calculated in eqn (1),<sup>28</sup> and the material composition share from Jain *et al.*<sup>29</sup> and Notten *et al.*<sup>28</sup> Welding, electricity use, heat consumption, and emissions during hull production are calculated according to

Notten *et al.*<sup>28</sup> The hull weight remains the same for each ship size while the propulsion systems are different.

$$\text{LWT} = (1 - 0.7) \times \frac{\text{DWT}}{0.7} \quad (1)$$

where LWT represents the weight of the empty vessel, including hull material, machinery, and outfitting;<sup>28</sup> deadweight tonnage (DWT) is the load capacity of the ship, including the cargo, fuel,

<sup>†</sup> This figure has been designed using images from Flaticon.com.



water, crew and effects;<sup>30</sup> and 0.7 is the ratio of the DWT to the total weight of the ship.<sup>31</sup>

**Propulsion system.** For each ship size, nine propulsion systems are modeled. Conventional diesel engines are used for the HFO-ICE propulsion system, while dual-fuel engines are used for ICEs fueled by LNG and H<sub>2</sub>-based fuels due to their ease of scaling up.<sup>3</sup> For ICE-based ships, the two-stroke slow-speed main engine drives the propeller directly *via* shafting, while a four-stroke medium-speed auxiliary engine is coupled with a generator to provide electricity. For dual-fuel LNG engines, there are two types: high-pressure engines with higher pilot fuel demand and low-pressure engines with lower pilot fuel demand but higher emissions of unburned methane.<sup>32</sup> In this study, the low-pressure type is chosen as it is the most widely adopted solution at present.<sup>33</sup> A small amount of diesel pilot fuel is required for these dual-fuel ICEs. For ICEs fueled by LNG and H<sub>2</sub>-based fuels, 1% and 5% of the energy content, respectively, is assumed to come from MGO.<sup>20,34</sup> To comply with the IMO Tier III NO<sub>x</sub> regulations, selective catalytic reduction (SCR) is assumed to be equipped for both the main and auxiliary engines in HFO-ICE, liquid NH<sub>3</sub>-ICE, and MeOH-ICE propulsion systems, while only the main engine is equipped with SCR in LNG-ICE, bio-LNG-ICE and liquid H<sub>2</sub>-ICE propulsion systems.<sup>20</sup> For fuel cells, PEMFC and SOFC are considered for the direct use of H<sub>2</sub> and NH<sub>3</sub>. The generated electricity powers the propeller *via* an electric motor and meets the auxiliary electrical and heating demands. Options such as cracking H<sub>2</sub>-based fuels to use H<sub>2</sub> in PEMFC are not considered due to

the additional onboard components required for cracking and purification, which would reduce overall system efficiency. The battery energy storage system is required to supply energy for the fuel cell's cold start-up, allowing the system to reach its operating temperature. For fuel cell-powered ships, the battery is sized to support 10 minutes of operation at 20% load for PEMFCs and 30 minutes at the same load for SOFCs.<sup>21</sup> This is because PEMFCs operate at a lower temperature than SOFCs, allowing for faster start-up and quicker response.<sup>35</sup> In this study, the battery depth of discharge is assumed to be 80%, with a 20% safety margin accounted for to consider battery degradation over its lifetime (11 years, requiring two replacements over a ship's 25-year lifespan). For the battery ship, Li-ion batteries are used to store grid electricity and power the ship in a manner similar to fuel cell ships. However, batteries are not suitable for long trips and are primarily used for short-sea shipping due to their lower energy density compared to other liquid fuels (*e.g.*, about 2% and 3% HFO's gravimetric and volumetric energy density, respectively).<sup>7</sup> The specific configurations of different propulsion systems are shown in Fig. S1 in the SI. For each ship size, alternative propulsion systems are sized to match the propeller and auxiliary system output power of the HFO-ICE propulsion system. For components with a lifespan shorter than the ship's service life, their replacement is taken into account. The key parameters and data sources for different components used in the propulsion systems are summarized in Table 1.

### 2.2.2. Fuel supply

**Fossil fuels and biofuels.** The HFO and MGO are sourced from the global market as modeled in the ecoinvent database.<sup>39</sup>

**Table 1** The main technical parameters of propulsion systems. In this table, 2S = two stroke, and 4S = four stroke, ICE = internal combustion engine, PEMFC = proton-exchange membrane fuel cells, SOFC = solid oxide fuel cells, DF = Dual fuel, and SCR = selective catalytic reduction

| Components   | Efficiency (%) | Lifespan (years) | Mass factor (t MW <sup>-1</sup> ) | Volume factor (m <sup>3</sup> MW <sup>-1</sup> ) | Key parameters source | LCI source |
|--|----------------|------------------|-----------------------------------|--|-----------------------|------------|
| 2S Diesel ICE                                      | 50             | 25               | 29.2                              | 27.5   | 21 and 36             | 21         |
| 2S LNG DFICE                                       | 50             | 25               | 29.2                              | 27.5   | 32 and 36             | 21         |
| 2S H <sub>2</sub> /MeOH DFICE                      | 48             | 25               | 29.2                              | 27.5   | 20 and 36             | 21         |
| 2S NH <sub>3</sub> DFICE <sup>a</sup>              | 46             | 25               | 29.2                              | 27.5   | 20 and 36             | 21         |
| PEMFC  | 55             | 6                | 3.3                               | 5.7  | 21 and 37             | 38         |
| SOFC   | 60             | 5                | 45.3                              | 97.2   | 21 and 37             | 21         |
| Li-ion battery                                     | 96             | 11               | —                                 | —  | 37                    | 39         |
| 4S Diesel ICE                                      | 48             | 25               | 29.2                              | 27.5   | 21 and 36             | 21         |
| 4S LNG DFICE                                       | 48             | 25               | 29.2                              | 27.5   | 32 and 36             | 21         |
| 4S H <sub>2</sub> /MeOH DFICE                      | 46             | 25               | 29.2                              | 27.5   | 20 and 36             | 21         |
| 4S NH <sub>3</sub> DFICE <sup>a</sup>              | 44             | 25               | 29.2                              | 27.5   | 20 and 36             | 21         |
| Alternator   | 96             | 25               | 2.5                               | 5  | 21 and 36             | 39         |
| Converter (main engine) <sup>b</sup>               | 98             | 25               | 2.3                               | 5.1  | 37 and 40             | 39         |
| Inverter   | 98             | 6                | 3.7                               | 9  | 41–43                 | 39         |
| Motor drive  | 97             | 25               | 1.1                               | 4.4  | 44–46                 | 47 and 48  |
| Electric motor                                     | 98             | 25               | 2.7                               | 4.2  | 21, 49 and 50         | 39         |
| Switchboard  | 99.8           | 11               | 0.7                               | 1.4  | 51–53                 | 39         |
| Converter (energy storage)                         | 98             | 25               | 3                                 | 6.7  | 37 and 40             | 39         |
| Shafting   | 99             | 25               | —                                 | —  | 54 and 55             | 28         |
| Exhaust gas/Oil composite boiler                   | 85             | 25               | 3                                 | 8.8  | 56 and 57             | 39         |
| Exhaust gas/Gas composite boiler                   | 85             | 25               | 3                                 | 8.8  | 56 and 57             | 39         |
| Exhaust gas/Electric composite boiler <sup>c</sup> | 99             | 25               | 3                                 | 8.8  | 57 and 58             | 59         |
| SCR  | —              | 25               | 0.9                               | 5  | 60 and 61             | 16         |

<sup>a</sup> In H<sub>2</sub>-based DFICE, NH<sub>3</sub> DFICE has a 2% lesser efficiency due to high heat of vaporization.<sup>21</sup> <sup>b</sup> This refers to fuel cells and Li-ion battery. <sup>c</sup> This type of boiler is installed on ICE ships powered by H<sub>2</sub>-based fuels. For fuel cell- and battery-powered ships, where a large flow of exhaust gas is unavailable, an electric boiler is required.



In this study, we further add a desulfurization process according to the study of Silva<sup>62</sup> to adapt the sulfur content in HFO and MGO from 1.03%<sup>39</sup> to 0.5% (very low sulphur fuel oil, or VLSFO) to satisfy the upper limit of sulfur content in fuel oil worldwide outside Sulphur Emission Control Areas (SECAs) under the IMO 2020 regulation.<sup>63</sup> Although a stricter sulfur content of 0.1% is regulated in SECAs,<sup>64</sup> and fuel oil switching may be required when ships are entering these areas, this process is not considered in this study, as the fuel used in SECAs is marginal compared to the total fuel consumption in container shipping. The regulation on sulfur content in marine fuels aims to reduce SO<sub>x</sub> emissions, as these emissions are solely determined by the sulfur content of the fuel used in ship operation, whereas NO<sub>x</sub> emissions are not only related to the nitrogen content in the fuel but can also be formed thermally from nitrogen and oxygen in the intake air at high engine temperatures.<sup>65,66</sup> The LNG is sourced from the global market as modelled in the ecoinvent database.<sup>39</sup> For bio-LNG production, gaseous synthetic biomethane with a pressure of 60 bar, derived from wood chips gasification using fluidized bed technology modeled in the ecoinvent database,<sup>39</sup> is further liquefied through a pressure reduction liquefaction facility.<sup>67</sup> Wood chips are sourced from sustainably managed forests.<sup>39</sup> The source and technology of biofuels used in maritime shipping are not specified in the IEA report.<sup>10,17</sup> Although there are other drop-in biofuels, such as Fischer-Tropsch biodiesel,<sup>10,68</sup> bio-LNG is used to represent biofuels due to its higher technology readiness.<sup>69</sup>

**H<sub>2</sub>-based fuels.** The supply of H<sub>2</sub>-based fuels is based on the global gaseous H<sub>2</sub> production model developed in our previous study Wei *et al.*,<sup>12</sup> which incorporates two H<sub>2</sub> production scenarios developed by the International Energy Agency (IEA): the Stated Policies (STEPS) Scenario and Net Zero Emissions by 2050 (NZE) Scenario.<sup>12</sup> These models cover nine leading H<sub>2</sub> production technologies, including coal gasification, natural gas steam reforming, and biomass gasification, both with and without carbon capture and storage (CCS), as well as grid-coupled water electrolysis using alkaline electrolyzers, proton exchange membrane electrolyzers, and solid oxide electrolysis cells. Additionally, the models account for electricity decarbonization, efficiency improvements, advancements in electrolyzer technology, and shifts in the H<sub>2</sub> production mix.

The gaseous H<sub>2</sub> from the global market<sup>12</sup> is used as the feedstock for the liquid H<sub>2</sub>, liquid NH<sub>3</sub> and MeOH production. The H<sub>2</sub> is liquefied in a liquefaction plant, consuming 10.5 kWh of electricity per kg of liquefied H<sub>2</sub>.<sup>70</sup> H<sub>2</sub> losses of 16.2 g per kg of liquid H<sub>2</sub> occur during this process.<sup>71</sup> The LCI is based on the research of Wulf and Zapp.<sup>71</sup> Liquid NH<sub>3</sub> is produced *via* the Haber-Bosch process by reacting gaseous H<sub>2</sub> with nitrogen obtained from cryogenic distillation. The LCI is derived from the research of D'Angelo, *et al.*<sup>14</sup> MeOH is synthesized from gaseous H<sub>2</sub> and captured CO<sub>2</sub> *via* direct air capture (DAC). DAC is currently operated in a few demonstration plants (TRL 6–7), with full commercialization expected by the late 2030s.<sup>24,72,73</sup> The LCI for MeOH production is based on the research of

González-Garay *et al.*<sup>74</sup> and Keith *et al.*<sup>75</sup> Although synthetic methane produced *via* the Sabatier reaction is also a type of synthetic H<sub>2</sub>-based fuel,<sup>76</sup> MeOH is used in this study as the representative since it is mainly covered in IEA reports.<sup>10,17,77</sup> Despite being at a similar TRL (9), synthetic methane may face commercial challenges given the low-cost availability of fossil gas and the growing production of biomethane.<sup>24</sup> Moreover, since synthetic H<sub>2</sub>-based fuels will account for only 0.5% of maritime fuel use by 2050 in the IEA's NZE scenario,<sup>10</sup> a more detailed differentiation between MeOH and synthetic methane would have only marginal impacts on the overall results.

### 2.2.3. Ship operation

**Energy demand for ship operation.** The energy demand for ship operation comes from the main engine power system, the auxiliary engine system, and the auxiliary boiler, which respectively satisfy propeller power, electricity use, and heating demand.<sup>3</sup> The energy demand for ship operation during a voyage is determined by the average output power and energy efficiency of the three systems, as well as by the operating time and fuel margin. It is calculated using eqn (2)–(4). The parameters required for each ship size are provided in Table S1 of the SI. A validation of our model has been conducted by comparing modelled direct CO<sub>2</sub> emissions of HFO ships with CO<sub>2</sub> emissions for each ship size category reported under the EU Monitoring, Reporting and Verification (EU-MRV) Maritime Regulation<sup>78</sup> and with calculated results presented in the IMO report.<sup>3</sup> Overall, both sets of measured values confirm the validity of our model for present-day ship emissions (see Section 3.1 of the SI for the detailed comparison).

$$E_{Oi} = \left( \frac{P_{OMi}}{\lambda_{MEi}} + \frac{P_{OAI}}{\lambda_{AEi}} + \frac{P_{OBI}}{\lambda_{ABSi}} \right) \times T \times FM \quad (2)$$

where  $E_{Oi}$  is the energy demand for the ship operation powered by propulsion system  $i$ , in MWh;  $P_{OMi}$  is the average output power of main engine in propulsion system  $i$ , calculated by the Admiralty formula (eqn (3));<sup>3</sup>  $\lambda_{MEi}$  is the energy efficiency for main engine in propulsion system  $i$ ;  $P_{OAI}$  is the average output power of the auxiliary engine in propulsion system  $i$ , calculated by eqn (4);<sup>79</sup>  $\lambda_{AEi}$  is the energy efficiency for auxiliary engine in propulsion system  $i$ ;  $P_{OBI}$  is the output power of the auxiliary boiler in propulsion system  $i$ , assumed equal to its installed power;  $\lambda_{ABSi}$  is the energy efficiency for auxiliary boiler system in propulsion system  $i$ . It should be noted that when the ship is at sea, the auxiliary boiler can utilize exhaust gas in ICE-based propulsion systems, while in fuel-cell-based propulsion systems, it requires electricity consumption.<sup>80</sup>  $T$  is the operation time for one voyage, determined by the voyage length and the average speed;  $FM$  is the fuel margin, which ensures voyage completion even in the event of potential detours, unexpected adverse weather conditions, or similar factors,<sup>7</sup> and is set to 1.2.<sup>81</sup>

$$P_{OMi} = \frac{P_{IMi} \times \left( \frac{d_{ave}}{d_{max}} \right)^{\left( \frac{2}{3} \right)} \times \left( \frac{v_{ave}}{v_{max}} \right)^3}{\eta_w \times \eta_f} \quad (3)$$



where  $P_{IMi}$  is the installed power of the main engine in propulsion system  $i$ ;  $d_{ave}$  and  $d_{max}$  represent the average and max draught of a ship in a specific voyage;  $v_{ave}$  and  $v_{max}$  represent the average and max speed of a ship in a specific voyage;  $\eta_w$  and  $\eta_f$  are correction factors for weather and fouling, indicating the power increase affected by weather conditions and hull fouling.

$$P_{Oai} = P_{Iai} \times l_{AE} \quad (4)$$

where  $P_{Iai}$  is the installed power of the auxiliary engine in propulsion system  $i$ ;  $l_{AE}$  is the load factor of the auxiliary engine, which is 0.5.<sup>79</sup>

**Energy demand for fuel storage.** For propulsion systems using LNG, liquid H<sub>2</sub> and liquid NH<sub>3</sub>, which are stored in cryogenic tanks on board, heat penetration can cause fuel evaporation, leading to the formation of boil-off gas (BOG).<sup>82</sup> The BOG can be managed by either directing it to the engine for propulsion or reliquefying it. However, the first method offers less control over the fuel consumption rate.<sup>82</sup> Therefore, in this study, BOG is conservatively assumed to be managed through a reliquefaction plant. As BOG decreases with fuel consumption, the reliquefaction capacity is designed based on the maximum BOG volume per hour. The mass and volumetric factors of the reliquefaction plant are 0.04 t and 0.11 m<sup>3</sup> per kilogram of liquefaction capacity per hour, respectively.<sup>83,84</sup> The additional energy required for this process is calculated using eqn (5):

$$E_{Ri} = \frac{k_{Ri}}{\lambda_{AESi}} \times \sum_{i=0}^{T-1} \left[ \left( \frac{E_{Oi}}{D_i} - \frac{E_{Oi} \times t}{D_i \times FM \times T} \right) \times BOG_i \right] \quad (5)$$

where  $E_{Ri}$  is the energy demand for reliquefying BOG, in MWh;  $k_{Ri}$  is the electricity demand for reliquefying BOG of propulsion system  $i$ , 1.23 kWh kg<sup>-1</sup> LNG,<sup>83</sup> 3.3 kWh kg<sup>-1</sup> liquid H<sub>2</sub><sup>85</sup> and 0.224 kWh kg<sup>-1</sup> liquid NH<sub>3</sub>;<sup>86</sup>  $\lambda_{AESi}$  is the efficiency of the auxiliary engine system for propulsion system  $i$ ;  $t$  is time point of ship operation in one voyage, in hours;  $D_i$  is the energy density for fuel used in propulsion system  $i$ ;  $BOG_i$  is the hourly evaporation rate of the fuel used in propulsion system  $i$ , 0.0054% per hour for LNG, 0.0167% per hour for liquid H<sub>2</sub> and 0.0017% per hour for liquid NH<sub>3</sub>.<sup>87</sup>

**Fuel storage.** Based on the energy demand for the trip, the tank size is further determined. HFO and MGO are stored in the diesel tank. MeOH, being liquid at atmospheric temperature, is stored in a carbon steel tank with epoxy coatings to prevent

corrosion. LNG, liquid H<sub>2</sub>, and liquid NH<sub>3</sub> are stored in cryogenic tanks, each with specific material requirements due to their differing storage temperatures. The related parameters for fuel storage and LCI data sources are shown in Table 2.

**Emissions of ship operation.** For each ship size, the gravimetric and volumetric changes of alternative propulsion systems and their corresponding fuel storage, compared to the conventional HFO-ICE system, are also quantified. The results are provided in the Section 1.3 of the SI. It should be noted that the gravimetric constraint directly affects cargo weight, while volumetric constraints, though significant, can be mitigated by mounting additional energy storage volume on deck.<sup>80,94,95</sup> Finally, fuel consumption per t-nm is determined based on energy demand, ship range, and resulting cargo weight. The fuel consumption and corresponding emissions for different propulsion systems are detailed in Table 3.

**2.2.4. Future transport demand for global container shipping.** Three scenarios, reflecting different ambitions for future containerized transport demand and the penetration of H<sub>2</sub>-based fuels, are explored in this study, as shown in Table 4. In setting these scenarios, consistency between socioeconomic development and energy scenarios is considered. The Less Ambitious scenario reflects current trends, where transport demand continues along historic trajectories, the penetration rate of H<sub>2</sub>-based fuels is extrapolated from the existing strategy, and H<sub>2</sub> production is modeled based on current policies. The Ambitious scenario envisions a society pursuing green growth, characterized by higher transport demand growth, with both the energy mix for container shipping and H<sub>2</sub> production aligned with net-zero CO<sub>2</sub> emissions targets. The Very Ambitious scenario explores a post-growth society placing greater emphasis on environmental sustainability and human well-being,<sup>100</sup> where transport demand grows more slowly, and container ship fleets transition more rapidly to fully renewable H<sub>2</sub>-based fuels. A detailed description is provided below.

In 2020, the transport demand of global container shipping was approximately 8.9 trillion t-nm.<sup>102</sup> Considering socioeconomic development across different pathways, future container shipping transport demand will follow varying patterns. Three social-economic development pathways are considered based on the Shared Socioeconomic Pathways (SSPs) and the Organization for Economic Co-operation and Development (OECD)'s long-term projections, as presented in the Fourth IMO GHG Study 2020:<sup>3</sup> SSP2, SSP1, and OECD. In SSP2, the

Table 2 The key technical parameters and data source of various fuels and their storage

| Fuel/energy storage    | Tank type                      | Lower heating value (MWh t <sup>-1</sup> ) | Gravimetric energy density including tank (MWh t <sup>-1</sup> ) | Volumetric energy density including tank (MWh m <sup>-3</sup> ) | Data source | LCI of tanks |
|------------------------|--------------------------------|--|--|---|-------------|--------------|
| HFO                    | Diesel tank                    | 11.2                                       | 9.7  | 11.1  | 19 and 88   | 89           |
| MGO                    | Diesel tank                    | 11.9                                       | 10.1   | 10.1  | 19          | 89           |
| LNG/Bio-LNG            | Cryogenic LNG tank             | 13.6                                       | 8.3  | 3.1   | 19          | 90           |
| Li-ion battery         | —                              | —  | 0.17   | 0.3   | 7           | —            |
| Liquid H <sub>2</sub>  | Cryogenic H <sub>2</sub> tank  | 33.3                                       | 5.6  | 1.3   | 19          | 91           |
| Liquid NH <sub>3</sub> | Cryogenic NH <sub>3</sub> tank | 5.2  | 4.2  | 2.9   | 19          | 90 and 92    |
| MeOH                   | MeOH tank                      | 5.6  | 4.6  | 4.4   | 19          | 89 and 93    |



**Table 3** Fuel consumption and emissions for different propulsion systems. Battery and liquid H<sub>2</sub>-PEMFC systems produce no emissions and are therefore not listed here

| Propulsion system  | HFO-ICE <sup>20,96–98</sup> |       | LNG/Bio-LNG-ICE <sup>20,34,96–98</sup> |         | Liquid H <sub>2</sub> -ICE <sup>16,20,96–98</sup> |        | Liquid NH <sub>3</sub> -ICE <sup>16,20,96–98</sup> |        | MeOH-ICE <sup>20,96–99</sup> |        | Liquid NH <sub>3</sub> -SOFC <sup>16</sup> |
|--|-----------------------------|-------|--|---------|---|--------|--|--------|------------------------------|--------|--|
|  | 2S                          | 4S    | 2S                                     | 4S      | 2S  | 4S     | 2S   | 4S     | 2S                           | 4S     | —  |
| Engine type  | 2S                          | 4S    | 2S                                     | 4S      | 2S  | 4S     | 2S   | 4S     | 2S                           | 4S     | —  |
| Main fuel (g kWh <sup>-1</sup> )                         | 178.6                       | 186.0 | 145.6                                  | 151.7   | 59.4  | 62.0   | 397.2  | 415.2  | 353.4                        | 368.8  | 320.5                                      |
| Pilot fuel (g kWh <sup>-1</sup> )                        | —                           | —     | 1.7                                    | 1.8     | 8.8   | 9.1    | 9.1  | 9.5    | 8.8                          | 9.1    | —  |
| Urea/NH <sub>3</sub> (g kWh <sup>-1</sup> ) <sup>a</sup> | 14.4                        | 9.6   | 14.4                                   | —       | 14.4  | —      | 8.2  | 6.6    | 14.4                         | 3.7    | —  |
| CH <sub>4</sub> (g kWh <sup>-1</sup> ) <sup>b</sup>      | 0.009                       | 0.009 | 4.4                                    | 4.5     | 0.0004  | 0.0004 | 0.0004   | 0.0004 | 0.0004                       | 0.0004 | —  |
| CO (g kWh <sup>-1</sup> )                                | 0.9                         | 1.0   | 1.2                                    | 1.2     | 0.2   | 0.2    | 0.2  | 0.2    | 4.1                          | 4.3    | —  |
| CO <sub>2</sub> (g kWh <sup>-1</sup> )                   | 585                         | 605   | 401                                    | 407     | 38  | 29     | 29   | 30     | 536                          | 551    | —  |
| NO <sub>x</sub> (g kWh <sup>-1</sup> )                   | 3.4                         | 2.6   | 3.4                                    | 0.7     | 3.4   | 0.7    | 3.4  | 2.6    | 3.4                          | 2.6    | 0.003                                      |
| N <sub>2</sub> O (g kWh <sup>-1</sup> )                  | 0.029                       | 0.030 | 0.014                                  | 0.014   | 0.001   | 0.002  | 0.013  | 0.014  | 0.001                        | 0.002  | —  |
| NH <sub>3</sub> (g kWh <sup>-1</sup> )                   | 0.026                       | 0.026 | 0.024                                  | 0.00002 | 0.024   | 0.0001 | 0.037  | 0.038  | 0.024                        | 0.024  | —  |
| NMVOG (g kWh <sup>-1</sup> )                             | 0.424                       | 0.441 | 0.446                                  | 0.465   | 0.024   | 0.025  | 0.025  | 0.026  | 0.021                        | 0.022  | —  |
| PM10 (g kWh <sup>-1</sup> )                              | 0.051                       | 0.053 | 0.003                                  | 0.003   | 0.003   | 0.003  | 0.003  | 0.003  | 0.011                        | 0.011  | —  |
| PM2.5 (g kWh <sup>-1</sup> )                             | 0.581                       | 0.605 | 0.035                                  | 0.037   | 0.029   | 0.031  | 0.031  | 0.032  | 0.123                        | 0.128  | —  |
| SO <sub>2</sub> (g kWh <sup>-1</sup> )                   | 1.795                       | 1.869 | 0.017                                  | 0.017   | 0.086   | 0.090  | 0.090  | 0.094  | 0.086                        | 0.090  | —  |
| CH <sub>2</sub> O (g kWh <sup>-1</sup> )                 | —                           | —     | —                                      | —       | —   | —      | —  | —      | 0.192                        | 0.200  | —  |

<sup>a</sup> In most propulsion systems, a 40 wt% urea solution (the urea amount is shown in the table) is used in the SCR to generate NH<sub>3</sub> for NO<sub>x</sub> reduction.<sup>34</sup> Excessive urea injection can lead to NH<sub>3</sub> slip, which is assumed to be 0.024 g per kWh.<sup>97</sup> However, in the liquid NH<sub>3</sub>-ICE system, the leaked NH<sub>3</sub> can be utilized as a reducing agent.<sup>20</sup> <sup>b</sup> For the LNG/Bio-LNG-ICE systems, a methane slip of 3 wt% is assumed during combustion.<sup>34</sup>

**Table 4** Scenarios for future container shipping demand and the propulsion system mix. In this table, non-fossil H<sub>2</sub> in the IEA's STEPS and NZE scenarios includes H<sub>2</sub> from water electrolysis and biomass gasification, with biomass gasification contributing only 0.09% and 0.27% of total gaseous H<sub>2</sub> production by 2050, respectively<sup>10,101</sup>

| Variables   | Less ambitious scenario <sup>3,4,12</sup>   | Ambitious scenario <sup>3,10,12</sup>   | Very ambitious scenario <sup>3,12</sup>  |
|---|---|---|--|
| Global container shipping demand                                | SSP2 pathway<br>• Higher: logistic model<br>• Lower: gravity model  | SSP1 pathway<br>• Higher: logistic model<br>• Lower: gravity model  | OECD pathway<br>• Higher: logistic model<br>• Lower: gravity model   |
| Fuel transition Penetration rate of H <sub>2</sub> -based fuels | IMO's 2023 strategy<br>• 2030-7.5%<br>• 2040-15%<br>• 2050-22.5%  | IEA's NZE scenario<br>• 2030-10%<br>• 2040-37%<br>• 2050-63%  | Own assumption<br>• 2030-33%<br>• 2040-67%<br>• 2050-100%  |
| Gaseous H <sub>2</sub> production mix                           | IEA's STEPS scenario  | IEA's NZE scenario  | 100% renewable electrolytic H <sub>2</sub> sourced from PEM with onshore wind power  |
| Propulsion systems  | • Non-fossil H <sub>2</sub> in 2020-0.04%<br>• Non-fossil H <sub>2</sub> in 2050-13.8%<br>• HFO-ICE<br>• LNG-ICE<br>• Liquid H <sub>2</sub> -ICE<br>• Liquid H <sub>2</sub> -PEMFC<br>• Liquid NH <sub>3</sub> -ICE<br>• Liquid NH <sub>3</sub> -SOFC<br>• MeOH-ICE | • Non-fossil H <sub>2</sub> in 2020-0.04%<br>• Non-fossil H <sub>2</sub> in 2050-61%<br>• HFO-ICE<br>• LNG-ICE<br>• Bio-LNG-ICE<br>• Battery<br>• Liquid H <sub>2</sub> -ICE<br>• Liquid H <sub>2</sub> -PEMFC<br>• Liquid NH <sub>3</sub> -ICE<br>• Liquid NH <sub>3</sub> -SOFC<br>• MeOH-ICE | • Non-fossil H <sub>2</sub> in 2020-100%<br>• Non-fossil H <sub>2</sub> in 2050-100%<br>• HFO-ICE<br>• LNG-ICE<br>• Liquid H <sub>2</sub> -PEMFC<br>• Liquid NH <sub>3</sub> -SOFC<br>• MeOH-ICE |

Middle of the Road narrative, socio-economic factors follow historical trends without significant shifts.<sup>103</sup> SSP1 envisions a world focused on green growth and sustainable development.<sup>104</sup> The OECD narrative has a lower gross domestic product (GDP) projection, leading to slower growth in transport demand.<sup>3</sup> At the same time, different prediction models, such as logistic and gravity models, estimate transport demand based on the elasticity of transport demand concerning per capita GDP and population. Projections using the logistic model typically show higher elasticity with respect to GDP compared to those based on the gravity model. Consequently, transport demand projections from the logistic model are about 45–83% higher in 2050 than those from the gravity

model.<sup>3</sup> This study presents both sets of results from the IMO's report,<sup>3</sup> with the difference between them representing the uncertainty inherent in projecting future developments. By 2050, container transport demand is projected to reach 16.9–25.6, 17.5–31.9, and 14.8–21.4 trillion t-nm in the Less Ambitious, Ambitious, and Very Ambitious scenarios, respectively. The transport demand by ship size from 2020 to 2050 is calculated based on the distribution of container ships across size categories, along with their cargo capacity and annual travel distance for each ship size. The distribution of ship numbers by size remains the same across different pathways.<sup>3</sup> In this analyses, we decided to build upon the existing, well elaborated scenarios discussed above. It is beyond the scope of this paper to work out our own, detailed



scenarios of future trade patterns. We acknowledge these may be needed given the recently introduced trade tariffs by the US, but given the high uncertainties in which tariffs in fact will be implemented, this would be an analysis in itself.

Correspondingly, different H<sub>2</sub> penetration rates, gaseous H<sub>2</sub> production mixes and propulsion systems are considered to align with various socio-economic development pathways. Currently, nearly all vessels are powered by HFO-ICE, while LNG-ICE accounted for only a tiny proportion (0.5%) as an alternative fuel.<sup>10,81,105</sup> In the Less Ambitious scenario, the 5–10% target for adopting zero or near-zero GHG emission fuels by 2030, as outlined in the IMO's revised GHG reduction strategy,<sup>4</sup> serves as the basis and is further explored linearly to 2050. The gaseous H<sub>2</sub> is sourced from the production mix in the IEA's STEPS scenario, which reflects the current policy setting. In the ambitious scenario, both the fuel mix for container shipping and the gaseous H<sub>2</sub> production mix from 2020 to 2050 are based on the IEA's NZE scenario. The ratios of liquid H<sub>2</sub>, liquid NH<sub>3</sub>, and MeOH in H<sub>2</sub>-based fuels in the Less Ambitious and Very Ambitious scenarios are set to be the same as those in the Ambitious scenario. For liquid H<sub>2</sub> and NH<sub>3</sub>, ICE and fuel cells will power the same transport demand in both the Less Ambitious and Ambitious scenarios. In the Very Ambitious scenario, a 100% penetration rate of H<sub>2</sub>-based fuels by 2050 is assumed. The gaseous H<sub>2</sub> is entirely sourced from water electrolysis powered by additional wind power capacity. For liquid H<sub>2</sub> and NH<sub>3</sub>, only fuel cells, which have a greater potential for GHG emissions reduction, will play a role. For each ship size, the same propulsion system share is assumed, except in the Ambitious scenarios, where the battery propulsion system is only applicable to the 0-999 TEU category with short-distance shipping routes.<sup>10,17</sup> The transport demand by ship size and propulsion system across three scenarios from 2020 to 2050 can be found in Section 2 of the SI.

**2.2.5. Background data.** To avoid the temporal mismatch between foreground and background data and to reflect the future development in other key sectors, this study uses prospective LCI background databases. These are derived from ecoinvent v3.8 database (system model "Allocation, cut-off by classification")<sup>39</sup> and the REMIND model,<sup>106</sup> utilizing the open-source Python library premise v1.5.8.<sup>107</sup> The REMIND model provides global future scenarios based on SSPs and representative concentration pathways. For the Less Ambitious, as well as Ambitious and Very Ambitious scenarios, two prospective LCI databases are used: SSP2-NDC (~2.5 °C warming by 2100) and SSP1-PkBudg500 (~1.3 °C warming by 2100). These databases update electricity inventories to reflect the regional electricity mix and efficiencies of various technologies, including CCS and photovoltaic panels.<sup>108</sup>

### 2.3. Life cycle impacts assessment

To quantify the climate change impact (kg CO<sub>2</sub>-eq), based on the IPCC AR5 characterization factors for global warming potentials with a 100-year time horizon,<sup>109</sup> we incorporate characterization factors for the uptake and release of biogenic CO<sub>2</sub> (−1 and +1, respectively), which are necessary for technologies such as

bioenergy with CCS (BECCS), and H<sub>2</sub> (+11), as H<sub>2</sub> can act as an indirect greenhouse gas.<sup>110</sup> Life cycle impact assessment results are calculated with the open-source software, Activity Browser.<sup>111</sup> The superstructure approach<sup>112</sup> is applied to handle LCA calculations with multiple foreground scenarios and prospective LCI background databases.

## 3. Results and discussion

### 3.1. Prospective GHG emissions of container shipping

Fig. 2 shows the GHG emissions of container ships powered by different propulsion systems, categorized by ship size and time, under the Less Ambitious, Ambitious, and Very Ambitious scenarios, respectively. In 2020, the GHG emissions of container ships powered by HFO ranged from 13 to 38 g CO<sub>2</sub>-eq per t-nm. Feeder ships, which operate in short-sea shipping, emit approximately three times more GHGs than Ultra Large Container Vessels (ULCVs). Compared to HFO, LNG results in a slight reduction in GHG emissions, ranging from 13 to 36 g CO<sub>2</sub>-eq per t-nm. Although LNG emits less CO<sub>2</sub> during combustion, the leakage of unburned methane during ship operation—around 30 times more potent than CO<sub>2</sub> over a 100-year time horizon—undermines its potential to mitigate climate change. In the future, the GHG emissions of both HFO- and LNG-powered ships are expected to remain largely unchanged across three scenarios.

Other alternative propulsion technologies show a clear change in GHG emissions over time. In the Ambitious scenario, although nearshore ships can be powered by batteries, the carbon intensity of the electricity source is critical to their decarbonization potential. In 2020, battery-powered feeder ships emitted 63 g CO<sub>2</sub>-eq per t-nm, as the global electricity mix was still largely dominated by fossil fuels. By 2050, near-zero-emission electricity enables battery-powered feeder ships to achieve just 3 g CO<sub>2</sub>-eq per t-nm, representing a 92% reduction in GHG emissions compared to HFO. Bio-LNG-powered ships emitted 8–22 g CO<sub>2</sub>-eq per t-nm across ship sizes in 2020, reducing GHG emissions by 30–42% compared to HFO. As the electricity used in the production and liquefaction of bio-LNG becomes increasingly decarbonized, the net GHG emissions of bio-LNG-powered ships decrease. However, methane leakage limits the overall GHG emissions reduction potential of bio-LNG. By 2050, the GHG emissions of bio-LNG-powered ships declines to 6–15 g CO<sub>2</sub>-eq per t-nm, representing a 55–58% reduction compared to HFO. Managing methane leakage is critical to maximizing the climate benefits of bio-LNG.

Due to variations in the H<sub>2</sub> production mix, the GHG emissions reduction potential of H<sub>2</sub>-based fuels differs across scenarios. In the Less Ambitious and Ambitious scenarios, H<sub>2</sub>-based fuels currently cannot reduce GHG emissions compared to fossil fuels, as H<sub>2</sub> production remains largely dependent on fossil fuels such as coal and natural gas. Based on the current H<sub>2</sub> market, liquid H<sub>2</sub>-ICE, liquid NH<sub>3</sub>-ICE and MeOH-ICE emit 24–68, 27–73, and 24–68 g CO<sub>2</sub>-eq per t-nm across various ship sizes, respectively. Fuel cell systems, due to their higher energy





Fig. 2 Prospective GHG emissions of different propulsion systems across various scenarios, by ship size and time. (a)–(d), (e)–(h), and (i)–(l) show the results for the Less Ambitious, Ambitious, and Very Ambitious scenarios, respectively. In these figures, H<sub>2</sub>-based fuels are sourced from the gaseous H<sub>2</sub> market. The red cross marker for battery mains is not applicable to ships with a capacity of 20 000+ TEU. Bio-LNG production and CO<sub>2</sub> capture through direct air capture can all contribute to negative emissions. The GHG emissions of different propulsion systems across various scenarios, by ship size from 2020 to 2050 in five-year intervals, are provided in Tables S293–S295 in the SI.

efficiency, offer lower GHG emissions: liquid H<sub>2</sub>-PEMFC and liquid NH<sub>3</sub>-SOFC emit 22–66 and 21–62 g CO<sub>2</sub>-eq per t-nm, respectively. For ships powered by liquid H<sub>2</sub> and NH<sub>3</sub>, in addition to the gaseous H<sub>2</sub> supply, the processes of H<sub>2</sub> liquefaction and NH<sub>3</sub> synthesis are significant contributors to GHG emissions due to their high electricity consumption. In the Less Ambitious scenario, despite electricity being decarbonized, the fossil-fuel-dominated H<sub>2</sub> market results in H<sub>2</sub>-based fuels having higher GHG emissions than HFO by 2050. In the Ambitious scenario, as the H<sub>2</sub> market adopts more CCS and water electrolysis, and electricity decarbonizes, H<sub>2</sub>-based fuels can reduce GHG emissions compared to HFO by 2050. The GHG emissions

of liquid H<sub>2</sub>-ICE, liquid H<sub>2</sub>-PEMFC, liquid NH<sub>3</sub>-ICE, liquid NH<sub>3</sub>-SOFC, and MeOH-ICE are expected to be 5–12, 4–10, 5–12, 4–10, and 6–15 g CO<sub>2</sub>-eq per t-nm, respectively. Compared to HFO in 2050, H<sub>2</sub>-based fuels sourced from the H<sub>2</sub> market can reduce GHG emissions by 52–68% for ULCVs and 58–73% for feeder ships. In the Very Ambitious scenario, where H<sub>2</sub>-based fuels are entirely produced using additional renewable electricity—including for gaseous H<sub>2</sub> production, liquefaction, NH<sub>3</sub> synthesis, direct air capture, and MeOH synthesis—the GHG emissions drop substantially. In 2020, liquid H<sub>2</sub>-PEMFC, liquid NH<sub>3</sub>-SOFC, and MeOH-ICE emit only 3–7, 3–8, and 5–11 g CO<sub>2</sub>-eq per t-nm, respectively, depending on ship size. This corresponds to a



63–74% reduction in GHG emissions for ULCVs and 70–82% for feeder ships, compared to HFO. These emissions can be further reduced by 2050, owing to the decarbonization of wind turbine manufacturing, to 2–5, 2–5, and 4–9 g CO<sub>2</sub>-eq per t-nm, respectively. This results in a 69–81% reduction in GHG emissions for ULCVs and 75–87% for feeder ships compared to HFO. Nonetheless, achieving this scenario remains highly challenging, as it necessitates a substantial expansion of renewable electricity capacity, amid competing demands from other electricity-intensive sectors beyond maritime shipping. As fuel consumption is the largest contributor to GHG emissions, a sensitivity analysis was also conducted to examine the effects of main engine efficiency, ship operation speed, voyage length and propulsion system mass on GHG emissions per t-nm. The results highlight that ship operating speed and main engine efficiency are the most important factors for reducing fuel consumption and thus GHG emissions (see Section 3.2 in the SI). It should be noted that the GHG emissions of new propulsion systems (excluding HFO-ICE and LNG-ICE) in 2020 should be regarded as benchmarks for assessing their changes over time, even though they were not yet deployed in the container ship fleet.

The GHG emissions of H<sub>2</sub>-based fuel propulsion systems, categorized by H<sub>2</sub> source, are further analyzed under the Ambitious scenario. As shown in Fig. 3, in 2020, regardless of whether CCS is applied, H<sub>2</sub>-based fuels produced through coal gasification or natural gas steam reforming result in higher GHG emissions than HFO. Similarly, due to the fossil-fuel-dominated electricity mix, H<sub>2</sub>-based fuels produced *via* water electrolysis using grid electricity also generate more than twice the GHG emissions of HFO. By 2050, utilizing gaseous H<sub>2</sub> from coal gasification and natural gas steam reforming with CCS to produce H<sub>2</sub>-based fuels can reduce GHG emissions by 5–32% and 24–47% for ULCVs, and by 12–36% and 31–52% for feeder ships, compared to HFO. This reduction is mainly attributed to the decarbonization of electricity used in H<sub>2</sub>-based fuel production, while the GHG emissions from gaseous H<sub>2</sub> produced by fossil fuels with CCS remain largely unchanged. In contrast, H<sub>2</sub>-based fuels produced *via* water electrolysis using grid electricity GHG emissions reduction potential similar to that of those sourced from fully renewable electricity. Only H<sub>2</sub>-based fuels derived from biomass gasification consistently reduce GHG emissions, and when combined with CCS, they can even achieve negative emissions. Compared to HFO, H<sub>2</sub>-based fuels from biomass gasification reduce GHG emissions by 12–39% for ULCVs and 22–46% for feeder ships in 2020. These reductions increase to 71–83% for ULCVs and 77–89% for feeder ships by 2050. Despite their substantial GHG reduction potential, biomass-derived H<sub>2</sub>-based fuels hold only a marginal market share both now and in future outlooks.<sup>10</sup>

### 3.2. Annual GHG emissions of global container shipping

In the future, the composition of ship fleets by size and propulsion system will evolve. We further quantify the impact of different scenarios regarding the penetration of H<sub>2</sub>-based fuels on annual GHG emissions at the fleet level. As shown in

Fig. 4, depending on the socio-economic pathway, container transport demand is projected to increase from 8.9 trillion t-nm in 2020 to 16.9–25.6, 17.5–31.9, and 14.8–21.4 trillion t-nm by 2050 under the Less Ambitious, Ambitious, and Very Ambitious scenarios, respectively. Across all scenarios, the share of large container ships (8000–11 999 TEU and above) is expected to expand. Their transport demand grows from 4.8 trillion t-nm in 2020 to 12.1–18.3, 12.5–22.8, and 10.6–15.3 trillion t-nm by 2050 in the three respective scenarios. In terms of fuel use, we assume the adoption of alternative propulsion technologies will begin in 2025. By 2050, transport demand powered by H<sub>2</sub>-based fuels is expected to reach 3.8–5.7, 11–20, and 14.8–21.4 trillion t-nm under the Less Ambitious, Ambitious, and Very Ambitious scenarios, respectively. In the Less Ambitious scenario, H<sub>2</sub>-based fuels will partially replace fossil fuels, though transport demand powered by HFO and LNG will still increase. In the Ambitious scenario, bio-LNG will power 3.6–6.6 trillion t-nm by 2050. Battery-electric propulsion will also contribute modestly to nearshore operations, undertaking 13–24 billion t-nm of transport demand. In the Very Ambitious scenario, liquid H<sub>2</sub>-PEMFC, liquid NH<sub>3</sub>-SOFC, and MeOH-ICE will power 10.8–15.6, 3.9–5.6, and 0.1–0.2 trillion t-nm of transport demand, respectively.

As a result, the GHG emissions of global container shipping were 199 Mt CO<sub>2</sub>-eq in 2020 and can reach 351–532, 160–291, and 46–67 Mt CO<sub>2</sub>-eq by 2050 under the Less Ambitious, Ambitious, and Very Ambitious scenarios, respectively. In the Less Ambitious scenario, the slower increase in annual GHG emissions after 2045 is mainly attributed to the expansion of larger vessels and the resulting reductions in fuel use and GHG emissions per t-nm, rather than the adoption of H<sub>2</sub>-based fuels. In contrast, by 2050, the replacement of HFO with H<sub>2</sub>-based fuels leads to an increase of 22–33 Mt CO<sub>2</sub>-eq. Despite supplying only 22.5% of transport demand, H<sub>2</sub>-based fuels will be responsible for 27% of total emissions. Although the IMO has proposed a decarbonization strategy, H<sub>2</sub>-based fuels will not reduce emissions in container shipping under an H<sub>2</sub> market shaped by existing policies, due to the high share of H<sub>2</sub> produced from fossil-based sources.

In the Ambitious scenario, by 2050, although global container shipping's transport demand is expected to increase two- to fourfold compared to 2020, the associated annual GHG emissions can be 0.8 to 1.5 times higher than the 2020 level. By replacing HFO with H<sub>2</sub>-based fuels and bio-LNG, GHG emissions can be reduced by 141–256 Mt and 40–73 Mt CO<sub>2</sub>-eq, respectively, by 2050. By that time, H<sub>2</sub>-based fuels and bio-LNG will contribute 46% and 19% of total emissions, respectively, while delivering 63% and 21% of transport demand. In the Very Ambitious scenario, adopting renewable H<sub>2</sub>-based fuels can drive immediate reductions in GHG emissions, even as transport demand continues to rise. By 2050, when global container shipping is fully powered by renewable H<sub>2</sub>-based fuels, it could reduce GHG emissions by 242–350 Mt compared to HFO. However, residual emissions will persist by 2050. BECCS may offer a potential solution for offsetting residual emissions; however, the availability of bioenergy





**Fig. 3** Prospective GHG emissions from H<sub>2</sub>-based propulsion systems for container ships in 2020 and 2050 by H<sub>2</sub> source in the Ambitious scenario. In this figure, CG = coal gasification, NG SMR = steam methane reforming of natural gas, BG = biomass gasification, CCS = carbon capture and storage, AE = alkaline electrolyzer, PEM = proton exchange membrane electrolyzer, and SOEC = solid oxide electrolysis cell. Gaseous H<sub>2</sub> production via biomass gasification with carbon capture and storage, and CO<sub>2</sub> capture through direct air capture can contribute to negative emissions. Prospective GHG emissions from H<sub>2</sub>-based ships by H<sub>2</sub> source under the Less Ambitious scenario are shown in Fig. S7 of the SI. In the Very Ambitious scenario, the H<sub>2</sub> market consists exclusively of 100% renewable electrolytic H<sub>2</sub> from PEM using newly built onshore wind power, without contributions from other technologies. Prospective GHG emissions from H<sub>2</sub>-based ships by H<sub>2</sub> source under the Very Ambitious scenario are the same as those shown in Fig. 2. To convey the information effectively, only the results for the smallest and largest ship categories in 2020 and 2050 are shown, as the outcomes for other ship categories and years fall within these ranges.



crops may be insufficient to meet ambitious carbon sequestration targets.<sup>113,114</sup> Moreover, large-scale deployment of BECCS entails significant social, economic, and environmental risks,<sup>115</sup> as bioenergy crop cultivation requires extensive land use, potentially affecting food security, water resources, and biodiversity.<sup>116–119</sup>



Fig. 4 Annual global container shipping transport demand and GHG emissions by ship size (a) and (b) and propulsion systems (c) and (d). In this figure, the stacked values are based on predictions from the logistic model. The yellow dashed lines represent the total annual transport demand and GHG emissions estimated by the gravity model for comparison.



In terms of ship size, vessels with capacities of 7999 TEU or less accounted for 46% of total transport demand and 59% of GHG emissions in 2020. By 2050, they would account for 28% of transport demand while contributing 36–40% of the sector's emissions across the three scenarios. At the same time, ships below 7999 TEU represent the largest share (>90%) of vessels older than 20 years by 2024.<sup>120</sup> Given these factors, this segment should be prioritized for the adoption of alternative propulsion technologies to maximize emission reduction potential if H<sub>2</sub>-based fuels can be produced in a low-carbon manner, as in the Ambitious and Very Ambitious scenarios. Retrofitting these older ships with alternative propulsion systems could provide a solution that extends their economic life and ensures competitiveness by complying with well-to-wake GHG emissions regulations (*e.g.*, the IMO Net-Zero Framework and FuelEU Maritime, taking effect from 2028—possibly later due to the delay in formal adoption in October 2025—and 2025, respectively) and avoiding penalties.<sup>121–123</sup> Fig. 5 further shows the temporal change in weighted average GHG emissions per t-nm of ship fleets by size across three scenarios. Depending on the penetration rate of H<sub>2</sub>-based fuel use, the decarbonization extent of H<sub>2</sub> production, and propulsion system choices, the weighted average GHG emissions per t-nm for the entire container shipping fleet decreases from 22 g CO<sub>2</sub>-eq in 2020 to 21, 9, and 3 g CO<sub>2</sub>-eq by 2050 under the Less Ambitious, Ambitious, and Very Ambitious scenarios, respectively. In 2020, the average GHG emissions per t-nm for different ship sizes ranged from 13 to

38 g CO<sub>2</sub>-eq. In the Less Ambitious scenario, the use of H<sub>2</sub>-based fuels can increase GHG emissions for each ship size, as H<sub>2</sub>-based fuels cannot be produced more cleanly than HFO. In the Ambitious scenario, the average GHG emissions per t-nm across different ship sizes in 2050 ranges from 6 to 15 g CO<sub>2</sub>-eq, representing a 53–59% decrease compared to 2020. In the Very Ambitious scenario, the gap in average GHG emissions per t-nm across different ship sizes narrows by 2050, with emissions decreasing by 81–86%, to a range of 2–5 g CO<sub>2</sub>-eq per t-nm.

### 3.3. Cumulative GHG emissions of global container shipping

To assess the role of the container shipping sector in achieving net-zero targets for the global economy, we further quantify its cumulative GHG emissions between 2020 and 2050. As shown in Fig. 6, the cumulative emissions are estimated to be 9–12, 7–10, and 4–5 Gt CO<sub>2</sub>-eq under the Less Ambitious, Ambitious, and Very Ambitious scenarios, respectively. In the Less Ambitious scenario, replacing HFO with H<sub>2</sub>-based fuels could increase cumulative emissions by 0.4–0.6 Gt CO<sub>2</sub>-eq. In contrast, in the Ambitious and Very Ambitious scenarios, H<sub>2</sub>-based fuels could reduce emissions by 1–2 and 3–5 Gt CO<sub>2</sub>-eq, respectively. Previous research estimates that the remaining global carbon budget for limiting warming to 1.5 °C with 67% certainty between 2020 and 2050 is approximately 400 (± 220) Gt CO<sub>2</sub>-eq.<sup>124</sup> Based on a 400 Gt CO<sub>2</sub>-eq budget, emissions from global container shipping could consume 1–3% of the total remaining carbon budget. In 2022, container shipping accounted



Fig. 5 Weighted average GHG emissions of ship fleet by size (TEU). In the figure, (a) represents the value in 2020, (b), (c), and (d) present the values for 2030, 2040, and 2050 in the Less Ambitious, Ambitious, and Very Ambitious scenarios, respectively.



for 26% of total CO<sub>2</sub> emissions from the maritime shipping sector, making it the largest contributor, next to bulk carriers (25%), and oil tankers (13%), as other important contributors.<sup>125</sup> We estimated that cumulative GHG emissions from the entire maritime shipping sector could use up 4–12% of the remaining carbon budget, posing a significant challenge to achieving net-zero targets by 2050. It should be noted that the cumulative GHG emissions from container shipping continue to rise after 2050 across all scenarios, further contributing to climate change. This underscores the urgent need for a rapid and transformative energy transition in maritime shipping to avoid overshooting the 1.5 °C target. For liquid NH<sub>3</sub>, concerns have been raised regarding toxicity as well as NO<sub>x</sub> and N<sub>2</sub>O emissions.<sup>126</sup> Although the technology has not reached market maturity, liquid organic H<sub>2</sub> carriers (LOHC), such as dibenzyltoluene, are currently being discussed as potential alternatives to liquid NH<sub>3</sub> for container shipping due to their lower toxicity and ability to be handled in a manner similar to diesel.<sup>71,127</sup> According to our analysis, deploying LOHC ships at scale instead of liquid NH<sub>3</sub> ships can slightly increase cumulative GHG emissions (see Section 3.4 of the SI).

### 3.4. Electrolyzer and electricity requirements for electrolytic H<sub>2</sub> use in container shipping

Decarbonizing container shipping with H<sub>2</sub>-based fuels depends on scaling up their production, especially *via* water electrolysis powered by low-carbon electricity. As shown in Fig. 7, in the Less Ambitious, Ambitious, and Very Ambitious scenarios,

the global container shipping sector requires approximately 40–49 Mt, 131–169 Mt, and 137–162 Mt of H<sub>2</sub>-based fuels annually by 2050. Most of this demand is met by liquid NH<sub>3</sub>, with volumes ranging from 30–46 Mt, 87–159 Mt, and 105–151 Mt, respectively. For comparison, current global NH<sub>3</sub> production is 201 Mt per year.<sup>128</sup> By 2050, NH<sub>3</sub> demand from container shipping alone will exceed half of today's production capacity under the Ambitious and Very Ambitious scenarios. A major expansion of NH<sub>3</sub> production capacity will be needed, as current output is primarily used for fertilizer.<sup>129</sup> The MeOH demand for container shipping will account for only around 1% of the current MeOH production capacity by 2050 under the Ambitious and Very Ambitious scenarios. However, the CO<sub>2</sub> demand from DAC may become a limiting factor for synthetic MeOH supply in container shipping. The current global DAC capture capacity is around 0.01 Mt CO<sub>2</sub>/year,<sup>130</sup> which would need to be expanded by a factor of 149 to 290 by 2050 to meet the CO<sub>2</sub> demand from container shipping alone under the Ambitious and Very Ambitious scenarios (see Fig. S10 in the SI).

To produce these H<sub>2</sub>-based fuels, the required gaseous H<sub>2</sub> production needs to reach 7–11 Mt, 20–37 Mt, and 25–36 Mt per year by 2050 in the three scenarios. Based on the H<sub>2</sub> composition assumed in each scenario, the electrolytic H<sub>2</sub> would account for 1–1.5 Mt, 12–23 Mt, and 25–36 Mt annually by 2050, respectively. In contrast, the global electrolytic H<sub>2</sub> production in 2023 was below 0.1 Mt.<sup>131</sup> This will require a significant ramp-up of electrolyzer capacity to produce the corresponding amount

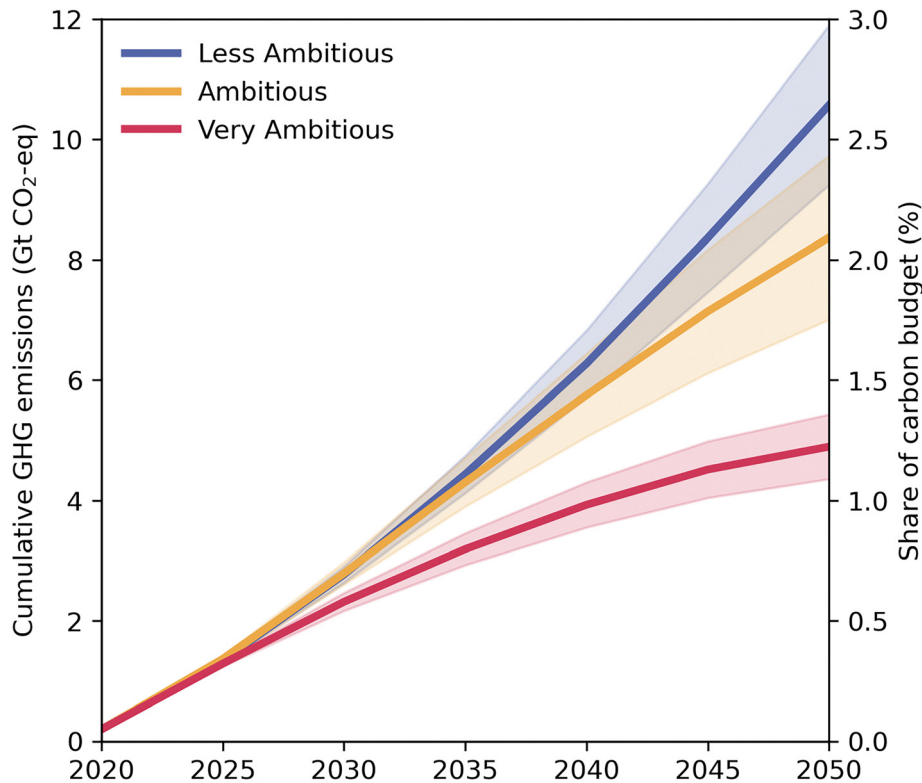


Fig. 6 Cumulative GHG emissions of global container shipping between 2020 and 2050 under the Less Ambitious, Ambitious, and Very Ambitious scenarios, and their share of the carbon budget for the 1.5 °C target. In this figure, the upper and lower boundaries of the range represent the values from the logistic and gravity models, respectively, while the line is the average value.





Fig. 7 Demand for (a) H<sub>2</sub>-based fuels, (b) electrolytic gaseous H<sub>2</sub>, (c) electrolyzer capacity, and (d) electricity required for electrolytic H<sub>2</sub> production in global container shipping under the Less Ambitious, Ambitious, and Very Ambitious scenarios. In this figure, the higher and lower boundaries represent the values corresponding to the transport demand estimated by the logistic and gravity models, respectively, while the line is the average value.

of electrolytic H<sub>2</sub>. In the Ambitious and Very Ambitious scenarios, electrolyzer capacity would reach 6–8 GW and 45–57 GW by 2030, and 80–146 GW and 173–250 GW by 2050, respectively. While the announced global electrolyzer capacity is expected to increase from 1.4 GW in 2023 to 230 GW by 2030,<sup>131</sup> not all of the announced electrolyzer projects may be installed and operational on time, creating a risk of a significant implementation gap.<sup>132</sup> For example, by the end of 2023, only 7% of the new capacity expected for installation in 2023 had been achieved.<sup>132</sup> Based on this, it is estimated that only 16 GW of electrolyzer capacity may be deployed by 2030. In the Ambitious scenario, the electrolyzer capacity required to decarbonize global container shipping will occupy half of this capacity, while in the Very Ambitious scenario, it will occupy three times as much. It is important to note that electrolyzer demand extends beyond maritime shipping, as it is also critical for decarbonizing other hard-to-abate sectors such as steel and chemicals. This presents a major obstacle to meeting the electrification and decarbonization targets for the maritime shipping sector.

In the Very Ambitious scenario, the large-scale production of renewable electrolytic H<sub>2</sub> could trigger an additional renewable electricity demand of around 1765 TWh by 2050. In total, including the electricity required for H<sub>2</sub>-based fuel production, approximately 2032 TWh of renewable electricity will be needed by 2050. Under current policy settings, low-emission electricity generation from sources such as solar PV, wind, hydropower, and nuclear is projected to increase by approximately 35 433 TWh between 2023 and 2050.<sup>133</sup> In this context, the renewable electricity demand for H<sub>2</sub>-based fuels would represent around 6% of the expected growth in low-emission electricity over this period. Given that renewable electricity is a competitive resource essential for decarbonizing the global economic sectors, sufficient capacity expansion is required.

## 4. Conclusions

In this study, we systematically assess the potential future climate change impact of global container shipping at both



the individual ship and fleet levels from 2020 to 2050. This assessment considers key drivers such as fuel mixes, propulsion systems, ship sizes, and future transport demand. The Less Ambitious, Ambitious, and Very Ambitious scenarios illustrate the varying roles of H<sub>2</sub>-based fuels in different maritime decarbonization roadmaps, integrating comparable energy transition and socio-economic development pathways. It should be noted that our scenarios are assessments of possible futures and ranges for emissions and not to be confused with predictions. Our findings provide insights for policymakers on the climate implications of adopting H<sub>2</sub>-based fuels in maritime shipping and highlight key challenges in realizing their decarbonizing potential. The main conclusions are as follows:

**H<sub>2</sub>-based fuels can substantially decarbonize maritime shipping, but clear policies are needed to prioritize those from low-carbon electrolysis over fossil-derived alternatives with CCS**

Currently, the immediate adoption of H<sub>2</sub>-based fuels fully sourced from renewables can enable rapid and deep decarbonization, reducing GHG emissions by over 80% per t-nm compared to HFO. This, however, requires additional renewable electricity capacity. Although H<sub>2</sub>-based fuels from biomass gasification with CCS also offer substantial GHG reduction potential, their limited scalability makes them a less promising option. As the power sector decarbonizes, H<sub>2</sub>-based fuels produced from grid electricity could achieve GHG reductions comparable to those from fully renewable sources by 2050. By then, H<sub>2</sub>-based fuels derived from fossil sources with CCS could offer at most a 50% reduction compared to HFO, primarily because the electricity used in their production would also be decarbonized, while the emissions from fossil-based gaseous H<sub>2</sub> with CCS would remain largely unchanged.

**The maritime shipping sector needs stronger policies to adopt renewable H<sub>2</sub>-based fuels, yet BECCS remains essential to achieving the net-zero target**

For global container shipping, transport demand is expected to increase two- to four-fold by 2050 compared to 2020. The sector still emits substantial amounts of GHG under all scenarios in 2050, with annual GHG emissions in 2050 ranging from one-quarter to three times the 2020 levels. Even if transport demand increases more slowly and is fully powered by renewable H<sub>2</sub>-based fuels, annual GHG emissions will still reach 56 Mt CO<sub>2</sub>-eq by 2050. It is estimated that the maritime shipping sector can still consume 4% of the global carbon budget remaining until 2050 to meet the worldwide net-zero target. Achieving net-zero emissions in the sector requires BECCS, but this approach is constrained by scalability limitations.

**Decarbonizing maritime shipping with H<sub>2</sub>-based fuels requires resolving major bottlenecks in fleet renovation, NH<sub>3</sub> production and electrolyzer capacity expansion, and renewable electricity supply**

As the current fleet still relies on conventional HFO-ICE propulsion systems, decarbonizing with H<sub>2</sub>-based fuels largely requires

retrofitting existing ships or inducing the entry of new ones. In the early stages, container ships with a capacity below 7999 TEU can be prioritized for adopting H<sub>2</sub>-based fuels, as they contribute a disproportionately high share of GHG emissions relative to their transport work and are relatively old, allowing for greater potential emissions reductions. As H<sub>2</sub>-based fuels are increasingly used to decarbonize maritime shipping, timely development and deployment of new NH<sub>3</sub> production and electrolyzer capacity are essential to ensure stable fuel supply and enable a smooth fleet transition. More importantly, sufficient renewable electricity is fundamental to maximizing the decarbonization potential of H<sub>2</sub>-based fuels in maritime shipping.

## Abbreviations

|                 |  |
|-----------------|--|
| AE              | Alkaline electrolyzers                                 |
| AIS             | Automatic Identification System                        |
| BECCS           | Bioenergy with carbon capture and storage              |
| BG              | Biomass gasification                                   |
| Bio-LNG         | Liquefied biomethane                                   |
| BOG             | Boil-off gas   |
| CCS             | Carbon capture and storage                             |
| CG              | Coal gasification                                      |
| GHG             | Greenhouse gas   |
| H <sub>2</sub>  | Hydrogen   |
| HFO             | Heavy fuel oil   |
| ICE             | Internal combustion engines                            |
| IEA             | International energy agency                            |
| IMO             | International maritime organization                    |
| LCA             | Life cycle assessment                                  |
| LCI             | Life cycle inventory                                   |
| LNG             | Liquefied natural gas                                  |
| LOHC            | Liquid organic H <sub>2</sub> carrier                  |
| MeOH            | Methanol   |
| MGO             | Marine gas oil   |
| NG SMR          | Steam methane reforming of natural gas                 |
| NH <sub>3</sub> | Ammonia  |
| NZE             | Net Zero Emissions by 2050 Scenario                    |
| OECD            | Organization for Economic Co-operation and Development |
| PEM             | Proton exchange membrane electrolyzers                 |
| PEMFC           | Proton-exchange membrane fuel cells                    |
| SCR             | Selective catalytic reduction                          |
| SOEC            | Solid oxide electrolysis cells                         |
| SOFC            | Solid oxide fuel cells                                 |
| SSPs            | Shared Socioeconomic Pathways                          |
| STEPS           | Stated Policies Scenario                               |
| ULCVs           | Ultra Large Container Vessels                          |

## Conflicts of interest

There are no conflicts to declare.



## Data availability

The data supporting this article have been included as part of the supplementary information (SI). Supplementary information is available. See DOI: <https://doi.org/10.1039/d5ee03477a>.

## Acknowledgements

The authors thank Karin van Kranenburg (TNO Vector) for sharing data on fuel storage, and Dr Fayas Malik Kanchiralla (Chalmers University of Technology) for sharing data on ship emissions. The authors also thank Xinpeng Jin (Leiden University) for his help with Adobe Illustrator. The authors also thank the anonymous reviewers for their constructive feedback. The authors further thank OpenAI's ChatGPT for its assistance in language polishing. This work is supported by the China Scholarship Council (Grant No. 202006430008).

## Notes and references

- UNCTAD, *Review of Maritime Transport 2023*, United Nations Conference on Trade and Development, Geneva, 2023.
- C. European Commission: Joint Research, M. Crippa, D. Guizzardi, E. Schaaf, F. Monforti-Ferrario, R. Quadrelli, A. Riquez Martin, S. Rossi, E. Vignati, M. Muntean, J. Brandao De Melo, D. Oom, F. Pagani, M. Banja, P. Taghavi-Moharamli, J. Köykkä, G. Grassi, A. Branco and J. San-Miguel, *GHG emissions of all world countries – 2023*, Publications Office of the European Union, 2023.
- IMO, *Fourth Greenhouse Gas Study 2020*, International Maritime Organization, London, 2021.
- IMO, *Revised GHG reduction strategy for global shipping adopted*, International Maritime Organization, London, 2023.
- S. Lagouvardou, B. Lagemann, H. N. Psaraftis, E. Lindstad and S. O. Erikstad, *Nat. Energy*, 2023, **8**, 1209–1220.
- J. Kersey, N. D. Popovich and A. A. Phadke, *Nat. Energy*, 2022, **7**, 664–674.
- B. Stolz, M. Held, G. Georges and K. Boulouchos, *Nat. Energy*, 2022, **7**, 203–212.
- IRENA, *A pathway to decarbonise the shipping sector by 2050*, International Renewable Energy Agency, Abu Dhabi, 2021.
- IMO, *Study on the readiness and availability of low- and zero-carbon ship technology and marine fuels*, International Maritime Organization, Didcot, 2023.
- IEA, *Net Zero by 2050-A Roadmap for the Global Energy Sector*, International Energy Agency, Paris, 2021.
- EC, Fit for 55, <https://www.consilium.europa.eu/en/policies/green-deal/fit-for-55/>, (accessed 29th, September, 2024).
- S. Wei, R. Sacchi, A. Tukker, S. Suh and B. Steubing, *Energy Environ. Sci.*, 2024, **17**, 2157–2172.
- K. de Kleijne, M. A. J. Huijbregts, F. Knobloch, R. van Zelm, J. P. Hilbers, H. de Coninck and S. V. Hanssen, *Nat. Energy*, 2024, **9**, 1139–1152.
- S. C. D'Angelo, S. Cobo, V. Tulus, A. Nabera, A. J. Martín, J. Pérez-Ramírez and G. Guillén-Gosálbez, *ACS Sustainable Chem. Eng.*, 2021, **9**, 9740–9749.
- Á. Galán-Martín, V. Tulus, I. Díaz, C. Pozo, J. Pérez-Ramírez and G. Guillén-Gosálbez, *One Earth*, 2021, **4**, 565–583.
- F. M. Kanchiralla, S. Brynolf, E. Malmgren, J. Hansson and M. Grahn, *Environ. Sci. Technol.*, 2022, **56**, 12517–12531.
- IEA, *Net Zero Roadmap: A Global Pathway to Keep the 1.5 °C Goal in Reach*, International Energy Agency, Paris, 2023.
- L. Van Hoecke, L. Laffineur, R. Campe, P. Perreault, S. W. Verbruggen and S. Lenaerts, *Energy Environ. Sci.*, 2021, **14**, 815–843.
- TNO, *E-fuels: Towards a more sustainable future for truck transport, shipping and aviation*, Netherlands Organisation for Applied Scientific Research, Delft, 2020.
- F. M. Kanchiralla, S. Brynolf and A. Mjelde, *Energy Environ. Sci.*, 2024, **17**, 6393–6418.
- F. M. Kanchiralla, S. Brynolf, T. Olsson, J. Ellis, J. Hansson and M. Grahn, *Appl. Energy*, 2023, **350**, 121773.
- M. Perčić, N. Vladimir, I. Jovanović and M. Koričan, *Appl. Energy*, 2022, **309**, 118463.
- M. Perčić, N. Vladimir and A. Fan, *Appl. Energy*, 2020, **279**, 115848.
- DNV, *Study on the readiness and availability of low- and zero-carbon ship technology and marine fuels*, Det Norske Veritas, Oxfordshire, 2023.
- AEA, Testing underway for 100 kW, direct ammonia SOFC, <https://ammoniaenergy.org/articles/testing-underway-for-100-kw-direct-ammonia-sofc/#:~:text=A%202%20MW%20version%20of,a%20role%20onboard%20the%20vessel>, (accessed 5th, September, 2025).
- SCHEEPVAARTWEST, <https://www.scheepvaartwest.be/CMS/index.php>, 2024).
- myShipTracking, <https://www.myshiptracking.com/>, 2024.
- P. J. Notten, H.-J. Althaus, M. Burke and A. Läderach, *Life cycle inventories of global shipping - Global*,ecoinvent Association, Zürich, 2018.
- K. P. Jain, J. F. J. Pruyn and J. J. Hopman, *Resour., Conserv. Recycl.*, 2016, **107**, 1–9.
- E. C. Tupper, in *Introduction to Naval Architecture*, ed. E. C. Tupper, Butterworth-Heinemann, Oxford, 2013, pp. 9–32, DOI: [10.1016/B978-0-08-098237-3.00002-3](https://doi.org/10.1016/B978-0-08-098237-3.00002-3).
- A. Papanikolaou, *Ship Design - Methodologies of Preliminary Design*, 2014.
- ICCT, *The climate implications of using LNG as a marine fuel*, International Council on Clean Transportation, Washington, DC, 2020.
- GR, *Review of Methane Slip from LNG Engines*, Green Ray, Espoo, 2023.
- S. Brynolf, M. Magnusson, E. Fridell and K. Andersson, *Transp. Res. D: Transp. Environ.*, 2014, **28**, 6–18.
- U.S.DOE, *Comparison of Fuel Cell Technologies*, U.S. Department of Energy, Washington, DC, 2016.
- MANES, *Marine engine programme-2nd edition 2023*, Man Energy Solutions, Augsburg, 2023.



- 37 K. Kim, G. Roh, W. Kim and K. Chun, *J. Mar. Sci. Eng.*, 2020, **8**, 183.
- 38 L. Usai, C. R. Hung, F. Vásquez, M. Windsheimer, O. S. Burheim and A. H. Strømman, *J. Cleaner Prod.*, 2021, **280**, 125086.
- 39 G. Wernet, C. Bauer, B. Steubing, J. Reinhard, E. Moreno-Ruiz and B. Weidema, *Int. J. Life Cycle Assess.*, 2016, **21**, 1218–1230.
- 40 ABB, Solar Inverters—ABB Medium Voltage Compact Skid (PVS-175-MVCS), ABB, Zurich, 2019.
- 41 E. Tazelaar, PhD, Technische Universiteit Eindhoven, 2013.
- 42 GPhilos, FUEL CELL INVERTER, [https://g-philos.co.kr/en/sub/product/fuel\\_cell\\_inverter\\_building.php#anc01](https://g-philos.co.kr/en/sub/product/fuel_cell_inverter_building.php#anc01), (accessed 10th, March, 2024).
- 43 ABB, Central Inverters—PVS800, 100 to 1000 kW, ABB, Zurich, 2014.
- 44 GEPC, MV6 Medium Voltage Drive-Leading next generation technology, GE Power Conversion, Paris, 2017.
- 45 RA, *PowerFlex 7000 Medium Voltage AC VFD—Air-Cooled*, Rockwell Automation, Milwaukee, 2024.
- 46 ABB, *Medium Voltage AC Drive ACS 5000, 1.5 MW–36 MW, 6.0–6.9 kV*, ABB, Zurich, 2013.
- 47 E. Westberg, Master, Linköping University, 2020.
- 48 ABB, ACS 6000 Medium Voltage AC drive for speed and torque control for power of 3 MW to 27 MW motors, ABB, Zurich, 2003.
- 49 S. Grzesiak, *New Trends Prod. Eng.*, 2018, **1**, 399–407.
- 50 HE, Induction Motors Medium & High Voltage, Hyundai Electric, Seongnam-si, 2019.
- 51 MAN-ES, *Diesel-electric Propulsion Plants: A brief guideline how to engineer a diesel-electric propulsion system*, MAN Energy Solutions, Munich, 2012.
- 52 EPD, Switchboard Maintenance: Safeguarding Your Electrical System's Longevity, <https://www.electronicpowerdesign.com/news/switchboard-maintenance/>, (accessed 12th, March, 2024).
- 53 SIEMENS, *Air-Insulated Medium-Voltage Switchgear NXAirS, up to 12 kV*, Shanghai, 2020.
- 54 MAN-ES, Basic principles of ship propulsion, MAN Energy Solutions, Copenhagen, 2018.
- 55 C. Guellec, C. Doudard, B. Leveil, L. Jian, A. Ezanno and S. Calloch, *Mar. Struct.*, 2023, **87**, 103325.
- 56 S. Sarco, Boiler Efficiency and Combustion, [https://www.spiraxsarco.com/learn-about-steam/the-boiler-house/boiler-efficiency-and-combustion?sc\\_lang=en-GB](https://www.spiraxsarco.com/learn-about-steam/the-boiler-house/boiler-efficiency-and-combustion?sc_lang=en-GB), (accessed 11th, February, 2025).
- 57 PARAT, *Marine Boilers*, Flekkefjord, 2024.
- 58 BOSCH, Electric steam boiler ELSB, <https://www.bosch-industrial.com/global/en/ocs/commercial-industrial/electric-steam-boiler-elsb-19175285-p/>, (accessed 5th, February, 2025).
- 59 A. M. A. Abbas, Master, An-Najah National University, 2015.
- 60 Y. Zhao, Y. Fan, K. Fagerholt and J. Zhou, *Transp. Res. D: Transp. Environ.*, 2021, **90**, 102641.
- 61 S. Shih-Tung, Master's thesis, University of Rostock, 2013.
- 62 M. Silva, Master, Norwegian University of Science and Technology, 2017.
- 63 IMO, *The 2020 global sulphur limit*, International Maritime Organization, 2021.
- 64 IMO, Ships face lower sulphur fuel requirements in emission control areas from 1 January 2015, International Maritime Organization, 2015.
- 65 J. Gao, S. Xing, G. Tian, C. Ma, M. Zhao and P. Jenner, *Fuel*, 2021, **285**, 119210.
- 66 EMSA, Possible Technical Modifications on Pre-2000 Marine Diesel Engines for NOx Reductions, European Maritime Safety Agency, 2008.
- 67 M. Gustafsson, I. Cruz, N. Svensson and M. Karlsson, *J. Cleaner Prod.*, 2020, **256**, 120473.
- 68 M. D. B. Watanabe, F. Cherubini and O. Cavalett, *J. Cleaner Prod.*, 2022, **364**, 132662.
- 69 I. Bioenergy, *The Role of Renewable Transport Fuels in Decarbonizing Road Transport: Production Technologies and Costs*, IEA Bioenergy Technology Collaboration Programme, Paris, 2020.
- 70 S. Z. S. Al Ghafri, S. Munro, U. Cardella, T. Funke, W. Notardonato, J. P. M. Trusler, J. Leachman, R. Span, S. Kamiya, G. Pearce, A. Swanger, E. D. Rodriguez, P. Bajada, F. Jiao, K. Peng, A. Siahvashi, M. L. Johns and E. F. May, *Energy Environ. Sci.*, 2022, **15**, 2690–2731.
- 71 C. Wulf and P. Zapp, *Int. J. Hydrogen Energy*, 2018, **43**, 11884–11895.
- 72 IEA, *Direct Air Capture—A key technology for net zero*, International Energy Agency, Paris, 2022.
- 73 F. Bisotti, K. A. Hoff, A. Mathisen and J. Hovland, *Chem. Eng. Sci.*, 2024, **283**, 119416.
- 74 A. González-Garay, M. S. Frei, A. Al-Qahtani, C. Mondelli, G. Guillén-Gosálbez and J. Pérez-Ramírez, *Energy Environ. Sci.*, 2019, **12**, 3425–3436.
- 75 D. W. Keith, G. Holmes, D. S. Angelo and K. Heidel, *Joule*, 2018, **2**, 1573–1594.
- 76 MAN-ES, SNG: Synthetic gas for the maritime transition, <https://www.man-es.com/marine/strategic-expertise/future-fuels/sng-biogas>, (accessed 5th September, 2025).
- 77 IEA, *The Role of E-fuels in Decarbonising Transport*, International Energy Agency, Paris, 2024.
- 78 EMSA, 2020-v207-23082025-EU MRV Publication of information, European Maritime Safety Agency 2025.
- 79 MAN, *Propulsion trends in container vessels*, MAN Energy Solutions, Copenhagen, 2024.
- 80 NCEMCT, *Life cycle assessment of maritime propulsion systems*, NCE Maritime CleanTech, Trondheim, 2020.
- 81 ICCT, *Refueling assessment of a zero-emission container corridor between China and the United States: Could hydrogen replace fossil fuels?*, International Council on Clean Transportation, Washington, DC, 2020.
- 82 C. J. McKinlay, S. R. Turnock and D. A. Hudson, *Int. J. Hydrogen Energy*, 2021, **46**, 28282–28297.
- 83 T. Park, S. So, B. Jeong, P. Zhou and J.-U. Lee, *J. Clean. Prod.*, 2021, **285**, 124832.



- 84 Wärtsilä, *Compact Reliq-Revolutionary Product Based on Proven Technology*, 2019.
- 85 H. Lee, Y. Shao, S. Lee, G. Roh, K. Chun and H. Kang, *Int. J. Hydrogen Energy*, 2019, **44**, 15056–15071.
- 86 J. Lee, Y. Choi and J. Choi, 2022, **10**.
- 87 Q. Song, R. R. Tinoco, H. Yang, Q. Yang, H. Jiang, Y. Chen and H. Chen, *Carbon Capture Sci. Technol.*, 2022, **4**, 100056.
- 88 MONJASA, Heavy Fuel Oil, Fredericia, 2017.
- 89 N. G. Dlamini, K. Fujimura, E. Yamasue, H. Okumura and K. N. Ishihara, *Int. J. Life Cycle Assess.*, 2011, **16**, 410–419.
- 90 J. M. Ryste, Master, Norwegian University of Science and Technology, 2012.
- 91 E. W. M. Abbas, Master, Chalmers University of Technology, 2022.
- 92 Cryocan, Ammonia Storage Tank, <https://cryocan.com/en/chemichal/ammonia-storage-tanks/>, (accessed 19th, December, 2024).
- 93 CGH, Methanol tanks, <https://cgh-rsa.co.za/tanks-for-the-industry/methanol-tanks>, (accessed 19th, December, 2024).
- 94 ABS, *Setting the Course to Low Carbon Shipping: View of the Value Chain*, American Bureau of Shipping, Texas, 2021.
- 95 IEA-AMF, Alternative Fuels for Marine Applications, International Energy Agency-Advanced Motor Fuels, Wiesenburg, 2013.
- 96 E. C. D. Tan, T. R. Hawkins, U. Lee, L. Tao, P. A. Meyer, M. Wang and T. Thompson, *Environ. Sci. Technol.*, 2021, **55**, 7561–7570.
- 97 K. Andersson and H. Winnes, *Proc. - Inst. Mech. Eng.*, 2011, **225**, 33–42.
- 98 EGCSA, NOx Reduction by Exhaust Gas Recirculation – MAN explains, <https://www.egcsa.com/exhaust-gas-recirculation-explained/>, (accessed 11th, June, 2024).
- 99 E. Malmgren, S. Brynolf, E. Fridell, M. Grahm and K. Andersson, *Sustainable Energy Fuels*, 2021, **5**, 2753–2770.
- 100 G. Kallis, J. Hickel, D. W. O'Neill, T. Jackson, P. A. Victor, K. Raworth, J. B. Schor, J. K. Steinberger and D. Ürgers-Vorsatz, *Lancet Planet. Health*, 2025, **9**, e62–e78.
- 101 IEA, *World Energy Outlook 2022*, International Energy Agency, Paris, 2022.
- 102 UNCTAD, *Review of Maritime Transport 2022*, United Nations Conference on Trade and Development Geneva, 2022.
- 103 O. Fricko, P. Havlik, J. Rogelj, Z. Klimont, M. Gusti, N. Johnson, P. Kolp, M. Strubegger, H. Valin, M. Amann, T. Ermolieva, N. Forsell, M. Herrero, C. Heyes, G. Kindermann, V. Krey, D. L. McCollum, M. Obersteiner, S. Pachauri, S. Rao, E. Schmid, W. Schoepp and K. Riahi, *Global Environ. Change*, 2017, **42**, 251–267.
- 104 K. Riahi, D. P. van Vuuren, E. Kriegler, J. Edmonds, B. C. O'Neill, S. Fujimori, N. Bauer, K. Calvin, R. Dellink, O. Fricko, W. Lutz, A. Popp, J. C. Cuaresma, S. Kc, M. Leimbach, L. Jiang, T. Kram, S. Rao, J. Emmerling, K. Ebi, T. Hasegawa, P. Havlik, F. Humpenöder, L. A. Da Silva, S. Smith, E. Stehfest, V. Bosetti, J. Eom, D. Gernaat, T. Masui, J. Rogelj, J. Streffler, L. Drouet, V. Krey, G. Luderer, M. Harmsen, K. Takahashi, L. Baumstark, J. C. Doelman, M. Kainuma, Z. Klimont, G. Marangoni, H. Lotze-Campen, M. Obersteiner, A. Tabeau and M. Tavoni, *Global Environ. Change*, 2017, **42**, 153–168.
- 105 HE, *How Hydrogen Can Help Decarbonise the Maritime Sector*, Hydrogen Europe, Brussels, 2021.
- 106 L. Baumstark, N. Bauer, F. Benke, C. Bertram, S. Bi, C. C. Gong, J. P. Dietrich, A. Dirnaichner, A. Giannousakis, J. Hilaire, D. Klein, J. Koch, M. Leimbach, A. Levesque, S. Madeddu, A. Malik, A. Merfort, L. Merfort, A. Odenweller, M. Pehl, R. C. Pietzcker, F. Piontek, S. Rauner, R. Rodrigues, M. Rottoli, F. Schreyer, A. Schultes, B. Soergel, D. Soergel, J. Streffler, F. Ueckerdt, E. Kriegler and G. Luderer, *Geosci. Model Dev.*, 2021, **14**, 6571–6603.
- 107 R. Sacchi, T. Terlouw, K. Siala, A. Dirnaichner, C. Bauer, B. Cox, C. Mutel, V. Daioglou and G. Luderer, *Renewable Sustainable Energy Rev.*, 2022, **160**, 112311.
- 108 P. Lamers, T. Ghosh, S. Upasani, R. Sacchi and V. Daioglou, *Environ. Sci. Technol.*, 2023, **57**, 2464–2473.
- 109 IPCC, *Climate Change 2013 – The Physical Science Basis: Working Group I Contribution to the Fifth Assessment Report of the Intergovernmental Panel on Climate Change*, Report 9781107057999, Intergovernmental Panel on Climate Change, Cambridge, 2013.
- 110 N. Warwick, P. Griffiths, J. Keeble, A. Archibald, J. Pyle and K. Shine, *Atmospheric implications of increased Hydrogen use*, Department for Business, Energy and Industrial Strategy, 2022.
- 111 B. Steubing, D. de Koning, A. Haas and C. L. Mutel, *Software Impacts*, 2020, **3**, 100012.
- 112 B. Steubing and D. de Koning, *Int. J. Life Cycle Assess.*, 2021, **26**, 2248–2262.
- 113 S. V. Hanssen, V. Daioglou, Z. J. N. Steinmann, J. C. Doelman, D. P. Van Vuuren and M. A. J. Huijbregts, *Nat. Clim. Change*, 2020, **10**, 1023–1029.
- 114 E. Kato and Y. Yamagata, *Earth's Future*, 2014, **2**, 421–439.
- 115 O. Y. Edelenbosch, A. F. Hof, M. van den Berg, H. S. de Boer, H.-H. Chen, V. Daioglou, M. M. Dekker, J. C. Doelman, M. G. J. den Elzen, M. Harmsen, S. Mikropoulos, M. A. E. van Sluisveld, E. Stehfest, I. S. Tagomori, W.-J. van Zeist and D. P. van Vuuren, *Nat. Clim. Change*, 2024, **14**, 715–722.
- 116 F. Creutzig, C. Breyer, J. Hilaire, J. Minx, G. P. Peters and R. Socolow, *Energy Environ. Sci.*, 2019, **12**, 1805–1817.
- 117 T. Hasegawa, S. Fujimori, S. Frank, F. Humpenöder, C. Bertram, J. Després, L. Drouet, J. Emmerling, M. Gusti, M. Harmsen, K. Keramidis, Y. Ochi, K. Oshiro, P. Rochedo, B. van Ruijven, A.-M. Cabardos, A. Deppermann, F. Fosse, P. Havlik, V. Krey, A. Popp, R. Schaeffer, D. van Vuuren and K. Riahi, *Nat. Sustainability*, 2021, **4**, 1052–1059.
- 118 V. Heck, D. Gerten, W. Lucht and A. Popp, *Nat. Clim. Change*, 2018, **8**, 151–155.
- 119 D. P. van Vuuren, E. Stehfest, D. E. H. J. Gernaat, M. van den Berg, D. L. Bijl, H. S. de Boer, V. Daioglou, J. C. Doelman, O. Y. Edelenbosch, M. Harmsen, A. F. Hof and M. A. E. van Sluisveld, *Nat. Clim. Change*, 2018, **8**, 391–397.



- 120 B. Bell, Ageing Fleet To Be Replaced By Massive Container Ship Orderbook, <https://www.brookesbell.com/news-and-knowledge/article/ageing-fleet-to-be-replaced-by-massive-container-ship-orderbook-159256>, (accessed 20th September, 2025).
- 121 UNCTAD, *Review of maritime transport 2024*, UN Trade and Development, Geneva, 2024.
- 122 DNV, *IMO Net-Zero Framework*, Det Norske Veritas, 2025.
- 123 DNV, *FuelEU Maritime*, Det Norske Veritas, 2025.
- 124 IPCC, *Climate Change 2022: Mitigation of Climate Change*, Intergovernmental Panel on Climate Change, Cambridge, UK and New York, NY, USA, 2022.
- 125 OECD, New estimates provide insights on CO<sub>2</sub> emissions from global shipping, <https://oecdstatistics.blog/2023/06/15/new-estimates-provide-insights-on-co2-emissions-from-global-shipping/>, (accessed 12th, December, 2024).
- 126 ISPT, *Clean Ammonia Roadmap*, Institute for Sustainable Process Technology, Amersfoort, 2024.
- 127 A. Peacock, B. Hull-Bailey, A. Hastings, A. Martinez-Felipe and L. B. Wilcox, *Int. J. Hydrogen Energy*, 2024, **94**, 971–983.
- 128 G. Eliseev, *The Ammonia Market Today and a Bridge to the Future*, S&P Global Commodity Insights, New Orleans, 2024.
- 129 IRENA, *Innovation Outlook: Renewable Ammonia*, International Renewable Energy Agency, Abu Dhabi, 2022.
- 130 IEA, Direct Air Capture, <https://www.iea.org/energy-system/carbon-capture-utilisation-and-storage/direct-air-capture>, (accessed 15th, September, 2025).
- 131 IEA, *Global Hydrogen Review 2024*, International Energy Agency, Paris, 2024.
- 132 A. Odenweller and F. Ueckerdt, *Nat. Energy*, 2025, **10**, 110–123.
- 133 IEA, *World Energy Outlook 2024*, International Energy Agency, Paris, 2024.

